

CHAPTER 1INTRODUCTIONThermodynamic Properties

Theories based on the initial Debye-Huckel approach to aqueous electrolytes have been successful only in the concentration region where the important forces governing the interactions are the long range electrical forces<sup>1</sup>. Extensions of these theories to concentrated solutions have failed because short range forces become important and, in many cases, predominant. The effects of these short range forces have been in many cases explained by hydration, complex ion formation and association but there still exist forces between molecules which cannot be explained along these lines.

To obtain a measure of the effects of these short range forces one could study the properties of nonelectrolytes in aqueous solutions but one is faced with the problem of the exact composition of the kinetic entities in the solution. The structure of the solute is often in doubt because of hydration and association. Interpretation of experimental results is further complicated because of the associated nature of water.

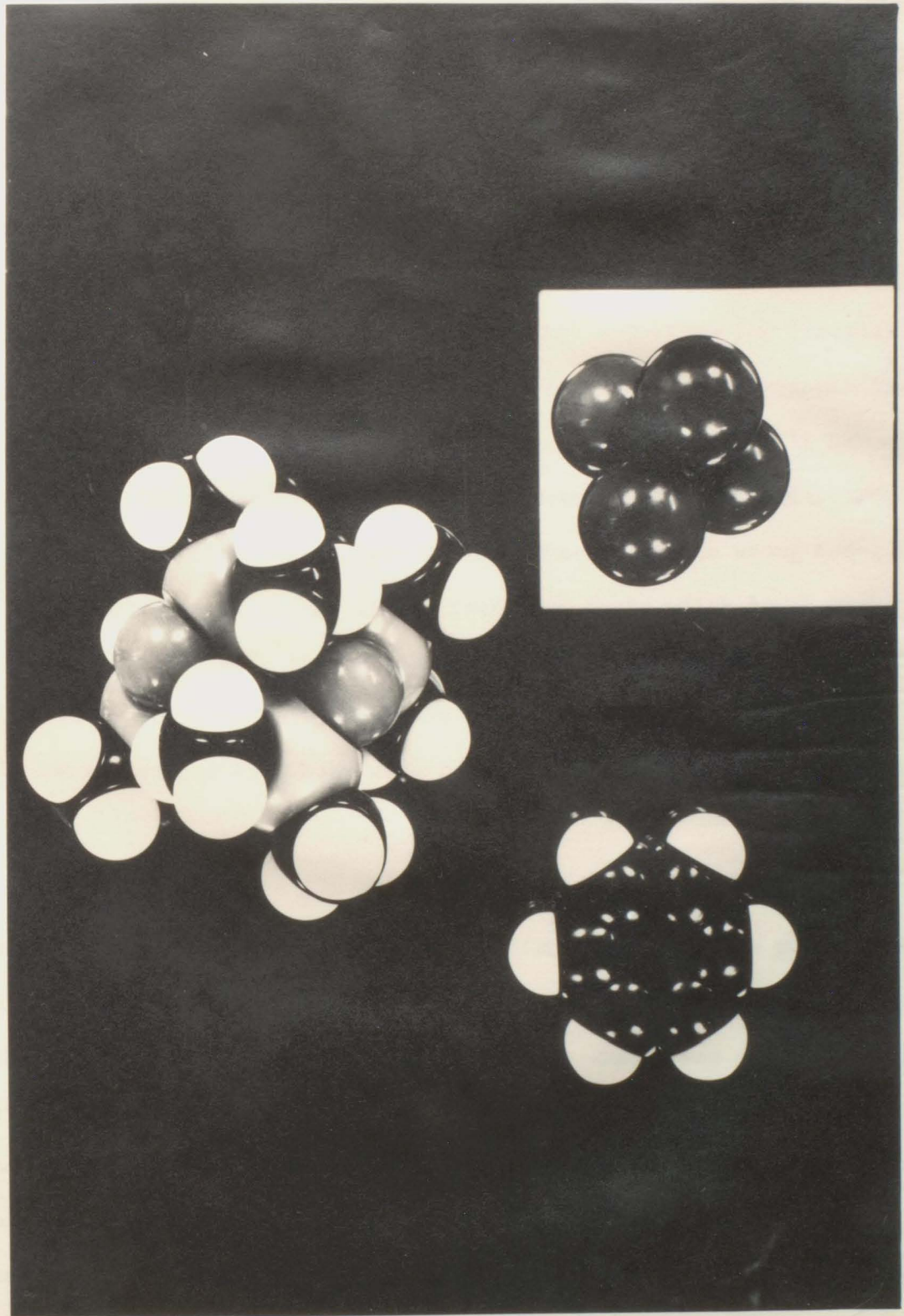
Research in this Department has been directed towards understanding the properties of both electrolytes and nonelectrolytes in moderately concentrated aqueous solutions. During these studies certain problems relating to the statistics of mixing have become apparent,

For example, if the solute molecule differs greatly in size from the solvent molecule, the question of the exact form of the statistics governing the entropy of mixing and the enthalpy of mixing becomes important. One requires to know if the mixing processes are governed by mole fraction, surface area fraction or volume fraction statistics or by something more complicated. One finds that these answers cannot be obtained from the various theories of liquid mixtures. It is obvious that theories must be guided by suitably devised experiments.

To provide answers to these questions it is necessary therefore to consider the properties of mixtures of nonpolar uncharged molecules where one knows what the kinetic species are. It is also advantageous to study systems where the size differences between the solute and the solvent are appreciable, so that one can readily distinguish between the various types of statistics. From a theoretical point of view, mixtures should be made from truly spherical molecules but such systems, for example the liquified rare gases, present many experimental difficulties. Because of the lack of experimental data on this type of system, the study of the systems mentioned in the abstract was undertaken. The properties of octamethylcyclotetrasiloxane have been discussed by Hildebrand<sup>2</sup>. The models of OMCTS, benzene and carbon tetrachloride are shown in Fig. 1.1.

It is constructive to consider the relative merits of the various theories of liquids and liquid mixtures. Theories based on the assumption that the liquid state has many features in common with a

Fig. 1.1



solid lattice can be applied to monomer - polymer mixtures because the polymer is allowed to occupy a number of lattice sites<sup>3,4,5,6</sup>. The use of such a model to treat mixtures of globular molecules differing greatly in size poses many problems. Moreover Hildebrand<sup>8,9,10</sup> has discussed the experimental facts which are inconsistent with any assumption of "lattice like" or "solid like" structure for liquids. Included in these facts are the dissimilarity of X-ray scattering diagrams of solids and liquids and the phenomenon of supercooling. It has also been shown that the cell model greatly overestimates the local order in liquids<sup>7</sup>. Hildebrand concludes that the use of the wrong model is not warranted, even though it predicts many facts which agree with experiment. The only theory based on a cell model that has been considered in this thesis is Barker's quasi-lattice theory<sup>11</sup>. In this theory allowances have been made for size differences between the two species.

Longuet-Higgins<sup>12</sup> has shown that properties of mixtures may be deduced from a knowledge of intermolecular forces and the properties of the pure components without having to resort to any particular model. The various theories based on this approach are termed corresponding state theories. Prigogine<sup>13</sup> has combined this approach with the cell model for liquids. His theory is only applicable to systems composed of molecules of approximately equal size<sup>14</sup>. Flory<sup>15</sup> has used an assumed form for the intermolecular energy suggested from considerations of the radial distribution function to calculate an equation of state

for liquid mixtures. This theory is applicable to the systems of interest.

Hildebrand has considered solutions from a less fundamental point of view.<sup>16</sup> His solubility parameter and regular solution concepts have been remarkably successful in connecting much of the entropy, solubility and enthalpy data on a variety of liquid mixtures. This theory makes no claims to being absolute, and improvements to the theory are restricted. As Hildebrand points out, "Further refinements will require something more basic than mere adjustment of the parameters. Any satisfying interpretation of liquids and solutions must be a molecular theory and involve molecular parameters"<sup>9</sup>.

In comparing solubility parameter predictions with the experimental results we have resorted to the adjustment of the parameters. Hildebrand concludes that the entropy of mixing is governed by mole fraction statistics while the enthalpy and volume of mixing is governed by volume fraction statistics but these conclusions are still open to doubt.

In recent years much attention has been paid to liquids and solutions composed of hard spheres. The most promising approach along these lines has been the scaled particle theory. In this theory a molecule is considered to possess a hard inner core and an outer soft shell. The volume of the molecule is determined by the soft core and the physical properties are determined by the hard core volume, or

more correctly, the reduced density given by the ratio of the hard core volume to the total volume. The equations of state derived by Lebowitz et al.<sup>17</sup> for a hard sphere liquid and for mixtures of hard spheres assumes that the intermolecular potential is zero outside the hard core and infinite inside the hard core. Yosim<sup>18</sup> has used these equations of state to calculate the excess entropy for a mixture of hard spheres.

Because the theory at the moment does not include a satisfactory intermolecular potential it cannot tell us anything about the excess enthalpy or the excess volume. Progress in this field is to be expected in the next few years.

### Transport Properties

As was the case with the thermodynamic properties, the interpretation of transport properties in aqueous solutions is complicated by the fact that the composition of the kinetic species is not known exactly and it is necessary to consider hydration, association and dissociation. These difficulties should be eliminated in mixtures formed from nonpolar molecules. Again one would expect more information from systems where the molecules differ in size.

An adequate theory of diffusion should explain the magnitude of the diffusion coefficient and the variation of the diffusion coefficient with concentration and in particular the relationship between the diffusion coefficient, the viscosity and the thermodynamic

properties of a mixture. Hartley and Crank<sup>19</sup>, Eyring<sup>20</sup>, Gordon<sup>21</sup> and Bearman<sup>22</sup> have suggested equations relating the above properties. Bearman<sup>22</sup> has shown that the first three equations are equivalent under certain conditions and that these equations are valid for the class of solutions where the radial distribution function is independent of composition. Bearman considers that these equations can only be expected to hold for liquid mixtures composed of nonpolar molecules of approximately equal size. Diffusion studies were initiated to test the above equations and to provide experimental data which could provide a guide to the formulation of new theories.

Details of the various theoretical approaches outlined above will be found elsewhere in this thesis.

CHAPTER 2EXPERIMENTAL TECHNIQUES2.1 INTRODUCTION

This chapter describes the experimental techniques used to study density, viscosity, mutual diffusion and activity coefficients in OMCTS-benzene and OMCTS-carbon tetrachloride mixtures.

Before considering the actual techniques, it is necessary to consider the degrees of purity required in the preparation of the various solutions. The criteria of purity of the components depend on the nature of the experiment performed. In the case of viscosity and diffusion the purity is not a critical factor<sup>23</sup> - it is only necessary to have a considerable stock of reasonably pure components. In contrast, the purity and outgassing of the components required for the vapour pressure measurements are quite critical. Purity requirements for density determinations depend on the type of experiment performed. Measurements of absolute densities require highly pure samples. When using density measurements to determine concentrations, the starting materials do not have to be as pure. The techniques used to purify and outgas the solvents will be discussed in detail.

Density, viscosity and mutual diffusion measurements involve routine and well-established experimental techniques. It is therefore unnecessary to describe them in great detail.

The determination of activity coefficients by the static vapour

pressure method involves a number of new techniques. As the literature is not well documented with details of absolute vapour pressure measurements on liquid mixtures, the apparatus and method will be described in full. A complete account of the construction and operation of the stainless steel diffusion cell is also included.

## 2.2 PURIFICATION OF MATERIALS

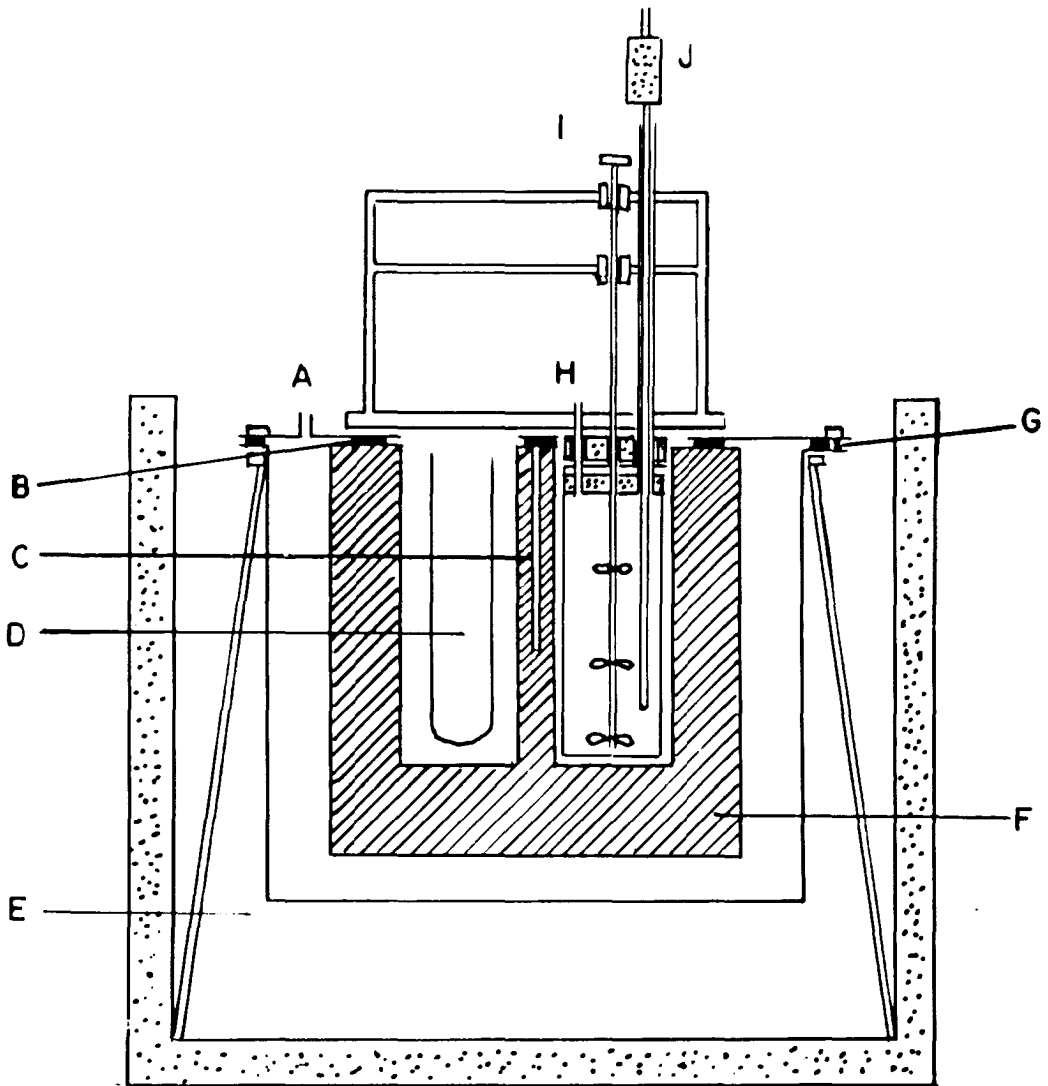
### Introduction

As previously noted, purity is not a critical factor to consider when measuring viscosity and mutual diffusion as only bulk properties are involved. Only small differences in results have been noted, even with a moderate amount of impurity present.<sup>23</sup> On the other hand, pure samples are required in activity coefficient work - one needs to measure vapour pressures and then consider deviations from ideal behaviour; hence the vapour pressure must be constant for all the samples used. For benzene, purity was determined by freezing point measurements, whilst for the other compounds constancy of the vapour pressures at a specific temperature for the first and last fractions were considered a sufficient criteria of purity.

### Freezing Point Apparatus

A schematic diagram of the freezing point apparatus is shown in Fig. 2.2.1. Cooling was achieved by a salt-ice mixture and the rate of cooling could be altered by variation of the pressure inside the inner container. The temperature of the sample was followed by a resistance

Fig. 2.2.1  
Freezing Point Apparatus



- |   |                  |   |                        |
|---|------------------|---|------------------------|
| A | Vacuum           | F | Aluminium Block        |
| B | Rubber Seal      | G | O - Ring               |
| C | Thermocouple     | H | Seeding Hole           |
| D | Drying Agent     | I | Stirrer                |
| E | Ice Salt Mixture | J | Resistance Thermometer |

thermometer, while the cooling rate of the aluminium block was monitored with a copper-constantan thermocouple connected to a one millivolt recorder. As the temperature of the sample approached the freezing point, resistance thermometer readings were taken every minute. The freezing point curve was followed until half the sample was frozen. Operation of the resistance bridge and thermometer are described in section 2.7.

The true freezing point was obtained by an extrapolation of the cooling curve data<sup>24,25</sup>. The apparatus shown in Fig. 2.2.1, incorporates certain design features to permit its later use for phase equilibrium studies.

#### Purification, degassing and drying apparatus

Samples required for vapour pressure measurements were prepared on the apparatus illustrated in Figs. 2.2.2 and 2.2.3. If a sample is introduced into the system shown in Fig. 2.2.2 at atmospheric pressure then the problem involved in degassing and regenerating the molecular sieve (which is used as the drying agent) are accentuated. It was found more convenient to introduce the sample under vacuum after it had been partially degassed.

#### Procedure

The sample (after the usual purification procedures to be described later) was distilled into apparatus B through the B14 cone. At this stage, B was connected to the vacuum line at D with the vacuum system

Fig. 2.2.2

Sample Preparing Apparatus (A)

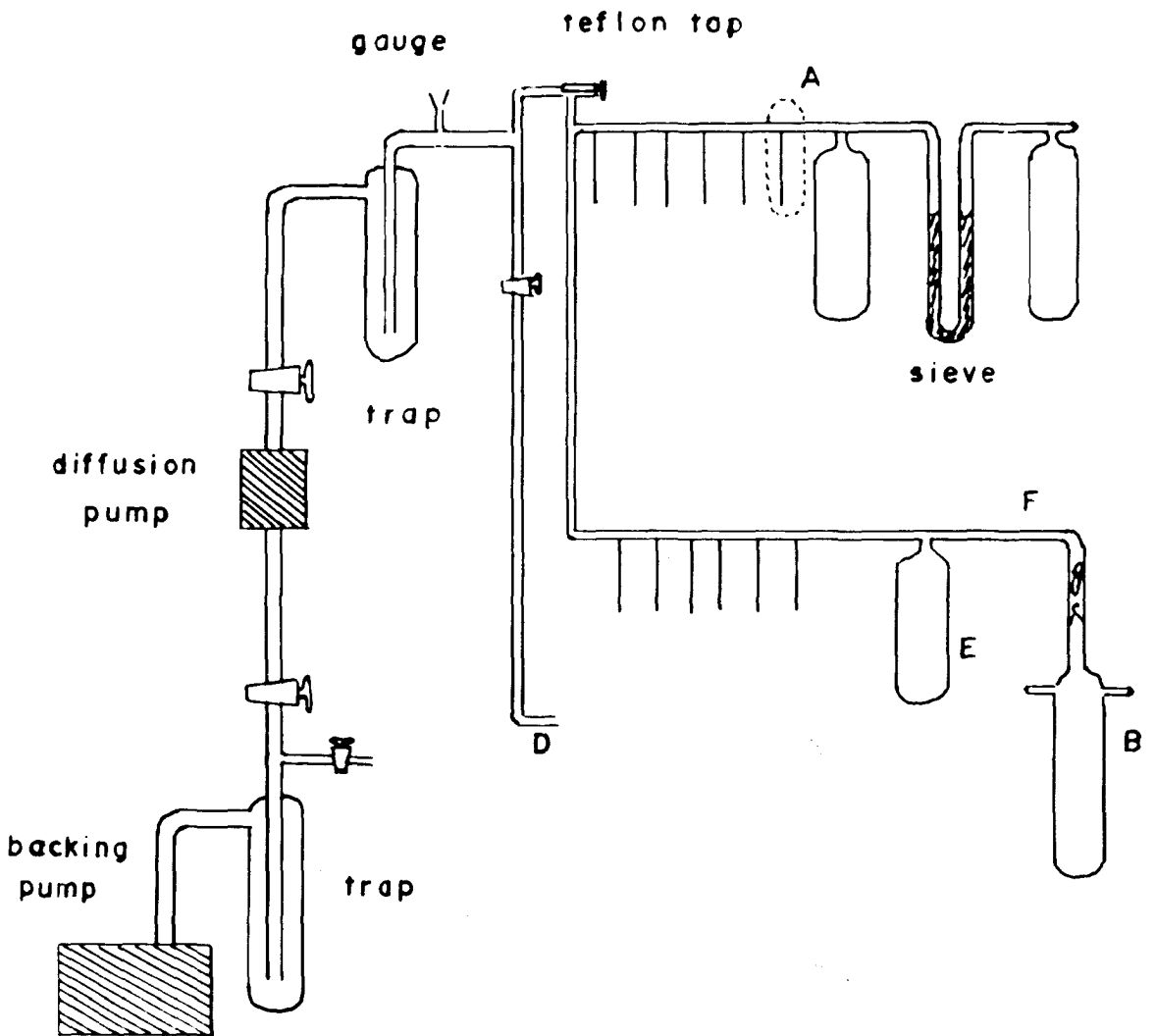
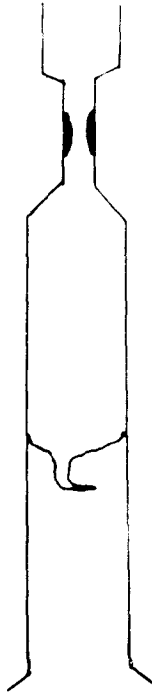


Fig 2.2.3

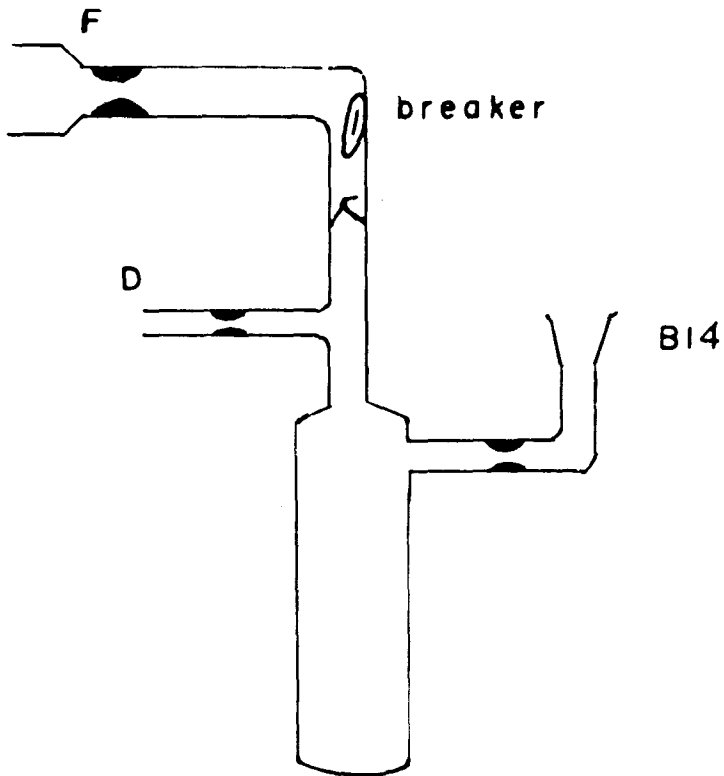
A



||  
constriction  
for sealing

breakseal

B



open to the air. At the completion of distillation the vacuum system was closed to air and the sample frozen in liquid air. Before freezing, the B14 socket was closed with a stopper to prevent condensation of moisture. The constriction below the B14 was then sealed and the apparatus evacuated.

The preliminary degassing stage was completed after melting, freezing and pumping the sample three or four times. The constriction at D was then sealed. The bulb B was sealed on to the sample-preparing line at F and the whole line evacuated. Over a period of a week the sample-preparation line was degassed by intermittent flaming with a torch. The drying agent was regenerated by heating at 250°C over several days. Linde molecular sieve type 4A, used as the drying agent, had pore sizes of approximately 4 Angstroms. This allowed water to be absorbed within the molecular mesh whereas the molecular sizes of benzene, carbon tetrachloride and OMCTS were such that they could not be absorbed. After a period of five days for degassing, the system was checked for leaks and desorption by means of a 0-0.005 mm Hg range Edwards Pirani gauge. If the pressure build-up was greater than 0.0005 mm Hg over a period of twelve hours, the process of flaming was continued.

A teflon tap was used as the only control tap to the sample-preparation line. By using this tap, the apparatus was completely grease-free, thus allowing it to be thoroughly flamed without the possibility of producing decomposition products. These teflon taps (Fischer and Porter) were specified to hold a vacuum to pressures less

than  $10^{-5}$  mm Hg. No leakages were experienced with any of these taps at any stage of their use.

After the degassing process was completed, the break seal on the bulb B was broken and the first few millilitres of the sample pumped away. The bulk of the 100-150 mls in the bulb was collected in E, using liquid air as the refrigerant. A residual 10 mls was frozen in bulb B before it was removed from the line by sealing at F.

The sample was then distilled back and forth through the molecular sieve using either liquid air or dry ice-acetone mixture as the condensing agent. McGlashan and Williamson<sup>26</sup>, Everett and Penney<sup>27</sup> and Baxendale et al.<sup>28</sup> have all stressed the necessity for pumping the sample in a dry ice-acetone mixture to remove the final traces of carbon dioxide. The final six distillations were completed with dry ice-acetone as the coolant.

The initial and final fractions from each distillation were generally discarded, reducing the final sample size to about half of the initial volume. It was found necessary to heat the molecular sieve to remove absorbed water. To complete this operation, the sample was distilled into the lower bulb and the U-tube containing the sieve was heated in a small furnace. To prevent desorbed water from condensing into the sample, the sample was kept at a temperature at which its vapour pressure was appreciable. This was achieved by ice-salt mixtures. With this technique, the water vapour could be pumped off and the possibility of back-diffusion into the sample prevented by the appreciable flow of sample vapour.

After the twelfth distillation, a portion of the sample was condensed into an ampoule. The liquid in both the storage bulb and the ampoule were frozen before the ampoule was sealed off, this precaution being necessary to prevent any decomposition of vapour during the sealing process. As a purity check the sample was distilled from the storage bulb into the ampoule from the liquid, and not the solid, state. Hence, proper distillation and not surface distillation was obtained. Sample purity was then determined by measuring the vapour pressures of initial and final samples.

Two experimental amendments were found necessary, Firstly, to prevent the molecular sieve from blowing out of the U-bend, small pieces of platinum gauze were pressed firmly down on the sieve. Secondly, to eliminate the possibility of an air leak in the event of the glass-enclosed metal breaker breaking, the metal was sealed into the glass under vacuum.

#### Summary

It is felt that the ampoule-preparing line described herein is superior to those previously employed. This conclusion is based on the following facts:

- (i) The glass surfaces may be adequately degassed.
- (ii) Water vapour may be adequately removed with in situ regeneration.
- (iii) The absence of grease joints (a disadvantage of most other apparatus). Note, however, the absence of these grease joints introduces another problem - the sample weight is not so easily determined, as will be seen in section 2.7.

Octamethylcyclotetrasiloxane purification

Distillation of the hydrolysis products of dimethyldichlorosilane yields OMCTS as the major constituent<sup>29,30</sup>. The OMCTS used in this work was a gift from the Silicone Division of the General Electric Corporation. The sample was labelled "> 99.9% purity" and gas-liquid chromatography indicated no impurities, so further purification of the original sample was considered unnecessary. Owing to the fact that only one litre was supplied in the gift sample, and the material was not available commercially, it was found necessary as experiments proceeded to recover as much as possible of the material and to develop techniques ensuring its most economical use.

After experiments ended, residues consisting of OMCTS diluted by large volumes of either carbon tetrachloride or benzene remained. The low-boiling fraction was removed by distillation. Density measurements on the crude samples always indicated a large concentration of impurities. The crude sample was distilled, subjected to repeated fractional crystallisations, then re-distilled, the purity being checked by density measurements. By repeating recovery procedures on the mother liquors losses were kept to a minimum. The purification method just described was for samples required for density, viscosity and diffusion work.

For OMCTS used in vapour pressure work, purification procedures were modified. A sample, purified as above, was subjected to three more fractional crystallisations, then distilled, recrystallised and dried over some activated molecular sieve. The techniques used for further

purification and degassing under vacuum have already been described.

Attempts were made to determine the freezing point of the OMCTS sample but owing to excessive supercooling, the major portion of the liquid solidified instantaneously. Seeding of the solution reduced, but did not eliminate, the supercooling. It would have been more convenient in this case to have followed the melting curve rather than the freezing curve. The estimated freezing point ( $17.50^{\circ}\text{C}$ ) compared favourably with the value recorded by Ostoff and Grubb ( $17.65^{\circ}\text{C}$ )<sup>31</sup>. Density measurements made during the final purification steps showed constancy but such a criterion of purity may not be good if impurities of a similar density are present.

#### Benzene purification

Purification of benzene stock for the density, viscosity and diffusion experiments was as follows: either B.D.H. or Hopkins and Williams "Analar" grade benzene was shaken with concentrated sulphuric acid until no colour appeared in the acid layer<sup>32</sup>. This process removed thiophene impurities. After washing several times with distilled water and drying over calcium chloride, the benzene was distilled. Owing to an atmospheric pressure of approximately 680 mm Hg at Armidale, the boiling temperature could be observed with a  $72\text{-}78^{\circ}\text{C}$  calorimeter thermometer which, with suitable magnification, could be read to  $0.001^{\circ}\text{C}$ . Fractions were collected over a boiling range of  $0.02^{\circ}\text{C}$  (after making corrections for the variations in atmospheric pressure). Normally a benzene stock of six litres was prepared and stored in a ten litre

flask. A syringe, fitted with a 15 inch long wide-bore stainless steel needle, was used to transfer material from the storage flask.

The benzene used for vapour pressure work needed to be of high purity. Its preparation has been described in the literature<sup>27,28,33</sup>. After treating eight litres of A.R. benzene as described in the preceding paragraph, the sample was fractionally recrystallised six times. Following the suggestion of Allen, Everett and Penney, the process of washing with sulphuric acid was repeated. The slight coloration noted was removed after the third washing. After washing with distilled water, drying and distilling, the sample was recrystallised a further three times, the freezing point being recorded after each recrystallisation. After the final one, the freezing point of the sample and the mother liquor agreed, but both were lower by approximately  $0.01^{\circ}\text{C}$  than literature values. This discrepancy may have been due to traces of water as no serious effort had been made to exclude moisture during freezing point measurements. It could not have been due to the lower atmospheric pressure at Armidale as the freezing point of benzene is lowered by only  $0.03^{\circ}\text{C}$  for a pressure decrease of one atmosphere<sup>33a</sup>. The variations of the freezing point of the sample with the number of recrystallisations are given in Table 2.2.1. After the final recrystallisation benzene was distilled and stored over carefully cleaned sodium wire.

TABLE 2.2.1.

Variation of freezing point of benzene sample with number  
of recrystallisations

Recrystallisation Number	Freezing Point (°C)
6	5.481
7	5.507
8	5.509
9	5.511
10	5.518
mother liquor	5.515

After recrystallisation number 10, both sample and mother liquor were distilled over sodium, directly into the freezing point apparatus.

Carbon tetrachloride purification

The carbon tetrachloride required for density, viscosity and diffusion measurements could be prepared by the one method. May and Baker, Hopkins and Williams and B.D.H. "Analar" grade carbon tetrachloride were all found to be suitable when once-distilled. Fractions were collected over a boiling range of 0.02°C.

Carbon tetrachloride used for vapour pressure work was subjected to more extensive purification. A sample was shaken over concentrated sulphuric acid, washed, refluxed for four hours over  $\text{KMnO}_4$  in 10% KOH and distilled<sup>34,35</sup>. After absorbing the water with calcium chloride and activated molecular sieve (Type 4A), the sample was fractionally distilled twice and recrystallised three times. Recrystallisations were

done in a 20 litre thermos cooled by several pounds of dry ice. The sample was finally distilled into a container connected to the degassing line and further purification was carried out as previously described.

#### Other materials

##### Potassium chloride

B.D.H. "Analar" grade potassium chloride, used for calibrating the stirred diaphragm diffusion cells and checking the operation of the Gouy diffusimeter, was employed without further purification.

##### Sucrose

Sucrose used for the calibration of the viscometer was twice recrystallised. For viscosity work it was essential that all suspended particles be removed. The process of filtering through a No.3 or No.4 porosity filter was found to be unsatisfactory owing to evaporation. Dust particles were removed from concentrated sucrose solutions by passing the solution through an eight inch column filled with small diameter Fenske glass helices. This method proved quite satisfactory.

##### Water

Aqueous solutions were prepared with deionised distilled water. The quality of the water was monitored continually by a method previously described<sup>36</sup>. This same water was used for the preparation of ice-water mixtures used to determine the ice-point of the resistance thermometer.

## Mercury

Mercury for use in the manometer was purified by the method described by McGlashan<sup>26</sup>, except that the air drying was carried out at room temperature and the mercury was distilled in vacuo in a triple still. It was distilled into the manometer under vacuum after thoroughly cleaning and flaming the manometer.

### 2.3 DENSITY DETERMINATIONS

#### Introduction

Density measurements were used for the determination of concentration, volume of mixing and purity. These therefore form an integral and necessary part of the experimental work; hence special efforts were made to ensure an accuracy approaching 0.001%.

Two types of pycnometers were used. For density measurements at 25°C conventional 27 ml Ostwald-Sprengel pycnometers, fitted with ground caps, were employed (Type I). A 55 ml flask type pycnometer, fitted with a 1 mm diam constant-bore capillary tube (Type II) was used for the higher temperature density measurements.

#### Calibration

Type I pycnometers were calibrated with water at 25°C; Type II at 25°, 35°, 45°, 55° and 60°. Densities of water at these temperatures were interpolated from the recent data of Kell and Whalley<sup>37</sup> which showed excellent agreement with the older data of Owen, White and Smith<sup>38</sup>.

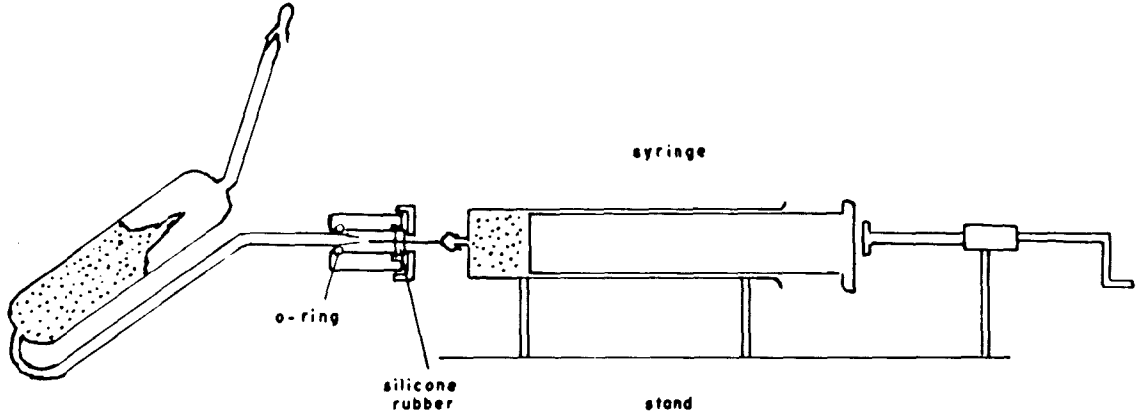
Discrepancies between the density data of water tabulated in the Handbook of Chemistry and Physics<sup>39</sup> and the more recent data, at temperatures above 55°C should be noted. The interpolated densities of water, at five degree intervals above 25°C, are tabulated in Table 2.3.1.

TABLE 2.3.1

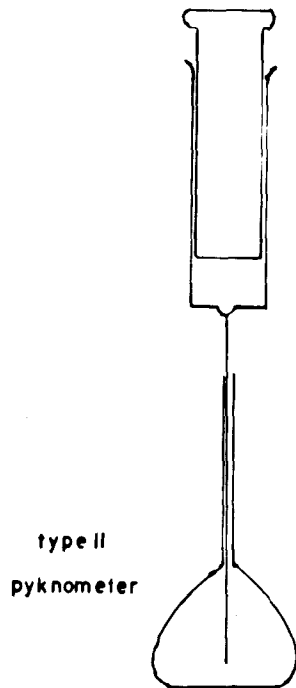
Temp (°C)	Density of water (g/ml )	Temp (°C)	Density of water (g/ml )
25	0.997075	65	0.980576
30	0.995677	70	0.977790
35	0.994062	75	0.974871
40	0.992246	80	0.971822
45	0.990243	85	0.968644
50	0.988065	90	0.965344
55	0.985721	95	0.961923
60	0.983222		

Type I pycnometers were used for routine determinations of concentrations and purity. They were filled from 50 ml and 30 ml syringes through an adaptor - see illustration in Fig. 2.3.1. To relieve hand fatigue, the syringe was placed on a stand and a hand-operated screw thread forced the plunger down the barrel. A Type II pycnometer was used to determine densities at the higher temperatures. To measure densities of mixtures at 25°C and 60°C, mixtures were made in situ by injecting the pure components directly into the flask using a syringe fitted with a fine gauge needle. The less volatile component was weighed in first, then the volatile component, the amount being sufficient to fill to a level just below the capillary. After weighing and mixing, the solution was equilibrated at 25°C and the liquid level

Fig. 2.3.1



type I  
pycnometer



was adjusted to near the reference mark on the capillary. The distance from liquid level to reference mark was determined with a cathetometer, and the appropriate correction to the final mass calculated from the known radius of the capillary and the density of the mixture. After weighing, the pyknometer was reimmersed at the higher temperature, equilibrated and the level readjusted.

### Analysis of Mixtures

Non-electrolyte mixtures may be analysed by the following methods:- density, refractive index, gas-liquid chromatography and complete fractionation. The first two are preferred methods owing to their simplicity. Since a suitably accurate routine method for refractive index measurement was not available, density measurement was adopted here.

This method proved ideal for the OMCTS-carbon tetrachloride mixtures, where the density difference between components was large - 0.634 g/ml. The accuracy in estimating the concentration in the OMCTS-benzene system was much less, owing to a small density difference - 0.077 g/ml.

Equations governing the relationship of concentration of a mixture to its density are developed below: symbol 1 represents OMCTS whereas symbol 2 refers to either carbon tetrachloride or benzene, i.e. the other component in any given mixture.

The ideal density  $\rho'$  is defined by,

$$\rho' = \frac{m_2 + m_1}{\frac{m_2}{\rho_2} + \frac{m_1}{\rho_1}} \quad \dots \quad (2.3.1)$$

m = mass,  $\rho$  = density.

The difference between the measured and the ideal density, ( $\Delta$ ) is given by,

$$\rho - \rho' = \Delta \quad \dots \quad (2.3.2)$$

$\rho'$  may be calculated from any mixture of known density, by interpolating  $\Delta$  from a graph of  $\Delta$  versus  $\rho$ .

#### Concentration in mole fractions

From equation (2.3.1),

$$m_2 = \frac{m_1(\rho'/\rho_1 - 1)}{1 - \rho'/\rho_2} \quad \dots \quad (2.3.3)$$

and

$$x_1 = \frac{m_1/M_1}{m_2/M_2 + m_1/M_1}$$

x = mole fraction, M = molecular weight.

whence,

$$x_1 = \left[ 1 + \frac{M_1 \rho_2 (\rho' - \rho_1)}{M_2 \rho_1 (\rho_2 - \rho')} \right]^{-1} \quad \dots \quad (2.3.4)$$

#### Concentration in moles per litre

$$c_1 = \frac{1000m_1/M_1}{(m_1 + m_2)/\rho}$$

c = concentration

From equation (2.3.3),

$$c_1 = 1000 \frac{\rho}{\rho'} \frac{\rho_1 (\rho_2 - \rho')}{(\rho_2 - \rho_1) M_1}$$

As an approximation,  $\rho \approx \rho'$  and therefore,

$$c_1 \approx \frac{1000}{M_1} \rho_1 \frac{(\rho_2 - \rho')}{(\rho_2 - \rho_1)} \quad \dots \quad (2.3.5)$$

### Volume fractions

$$\phi_1 = \frac{m_1/\rho_1}{m_1/\rho_1 + m_2/\rho_2}$$

$\phi$  = volume fraction.

From (2.3.3)

$$\phi_1 = \frac{\rho_2 - \rho'}{\rho_2 - \rho_1} \quad \dots \quad (2.3.6)$$

This equation gives the volume fraction for an ideal mixture.

### Excess volume

$$-V^E = \frac{x_1 M_1}{\rho_1} + \frac{x_2 M_2}{\rho_2} - \frac{(x_1 M_1 + x_2 M_2)}{\rho} \quad \dots \quad (2.3.7)$$

$V^E$  = excess volume.

### Corrections involved in density measurements

#### Vacuum corrections

The weight of a solution was corrected to a weight in vacuo by,

$$W_{\text{vac.}} = W_{\text{air}} \left( 1 + \rho_a \left( \frac{1}{\rho} - \frac{1}{\rho_w} \right) \right) \quad \dots \quad (2.3.8)$$

$\rho_a$  = density of air,  $\rho$  = density of solution at weighing temperature,

$\rho_w$  = density of weights.

The air density was read from a group of graphs drawn up from

$$\rho_a = \frac{0.001293 (P - k)}{(1 + 0.0036t)760} \quad \dots \quad (2.3.9)$$

P = pressure in mm Hg, t = temperature in degrees Centigrade, and k is a correction related to the humidity H by

$$k = 0.0038 H P_{H_2O}^t$$

$P_{H_2O}^t$  = vapour pressure of water in mm Hg<sup>40</sup>.

For each one degree interval between 17° and 27°C, graphs of  $\rho_a$  against P were constructed for 50% and 80% humidity. The term  $(\frac{1}{\rho} - \frac{1}{\rho_w})$  was calculated for each solution.

#### Vapour corrections

As weighings were carried out at temperatures below bath temperatures, the weighed solution occupied a smaller volume than the calibrated volume of the pycnometer. The volume difference consisted of air saturated with the volatile component. This process can be pictured as the displacement of an amount of air equal to the amount of volatile component above the solution, and is given by,

$$m = \frac{P_2 \Delta V \rho_a}{P} \quad \dots (2.3.10)$$

$P_2$  = partial pressure of the volatile component at weighing temperature, P = atmospheric pressure and  $\Delta V$  = volume change when the solution cools from equilibration temperature to room temperature.

The vapour pressure correction was negligible for all measurements at 25°C, but significant for temperatures above 50°C - the density correction to benzene at 60°C was  $1.1 \times 10^{-5}$  g/ml.

Further vapour corrections

A more subtle correction term, arising from the consideration of evaporation during the filling process, is needed. Density determinations were made by preparing mixtures in a 70 ml or 100 ml Quickfit flask. By weighing in the less volatile component first and adding sufficient of the volatile component to just fill the flask, vapour space corrections were eliminated. The prepared mixture was then injected into a pyknometer using a syringe. Initially, the pyknometer was filled with air, but during the filling process the air space would become saturated with the vapour of the volatile component. On filling, the saturated air would be forced out. The assumption that rapid saturation of the air space occurred was justified as a considerable stream of liquid emerged from the capillary filling arm. The mass of volatile component lost is given by,

$$m = \frac{p_2^0 \times x_2 M_2 v}{RT} \quad \dots (2.3.11)$$

$p_2^0$  = vapour pressure of component 2 at filling temperature,  $x_2$  = mole fraction of 2,  $M_2$  = molecular weight, and  $v$  = volume of pyknometer.

This equation assumes (i) saturation of the vapour space immediately the filling process begins and (ii) ideal behaviour in both the gas and the liquid phase.

In this evaporation process, a volume  $m/\rho_2$  is lost. Imagine that the lost benzene is restored to the solution by increasing the volume of the pyknometer by an amount  $m/\rho_2$ . The solution in the imaginary pyknometer

will have the same composition as that made up in the flask.

The mass of liquid in the imaginary pyknometer,  $m_I$ , is given by,

$$m_I = m_w + m$$

$m_w$  = mass of liquid in real pyknometer.

The volume of imaginary pyknometer,  $v_I$ , is then,

$$v_I = v + m/\rho_2$$

$$\begin{aligned} \rho_{\text{true}} &= m_I/v_I \\ &= \frac{m_w + m}{v(1 + m/v\rho_2)} \\ &= \frac{m_w(1 + m/m_w)}{v(1 + m/v\rho_2)} \end{aligned}$$

Neglecting the square terms,

$$\rho_{\text{true}} = \rho_{\text{meas.}} \left( 1 + \frac{m}{m_w} - \frac{m}{v\rho_2} \right)$$

therefore,

$$\rho_{\text{true}} = \rho_{\text{meas.}} + \rho_{\text{meas.}} \cdot m \left( \frac{1}{m_w} - \frac{1}{v\rho_2} \right)$$

$$m_w = v\rho_{\text{meas.}},$$

$$\rho_{\text{true}} = \rho_{\text{meas.}} + \frac{m}{v\rho_2} (\rho_2 - \rho) \quad \dots \quad (2.3.12)$$

where  $\rho_2$  = density of volatile component,  $\rho$  = density of mixture at equilibration temperature and  $v$  = volume of pyknometer.

The above approach assumes that only benzene is volatile. Though OMCTS is less volatile, its molecular weight is much higher. The ratio of OMCTS to benzene in the vapour space is given by,

$$R = m_1/m_2$$

$$= \frac{p_1^0 x_1 M_1}{p_2^0 x_2 M_2}$$

As an example, at a mole fraction  $x_1 = 0.95$ , the masses of OMCTS and benzene in the vapour space are equal. At mole fraction  $x_1 < 0.90$ , the mass of OMCTS is negligible compared with the mass of benzene.

The magnitude of this correction term will be discussed in the section on results. It may be eliminated by preparing solutions in situ in a Type II pyknometer if the involatile component is weighed in first. The term, therefore, was only considered when calculating excess volumes - it was unnecessary when making concentration determinations from density measurements.

## 2.4 VISCOSITY DETERMINATIONS

### Introduction

In order to interpret the equations relating diffusion and viscosity, it was necessary to measure the viscosity over the same temperature and concentration range for which diffusion was studied.

The kinematic viscosity was measured in a standard Ostwald-type viscometer - hence the following outline applies to that instrument.

Ideal flow through a capillary tube is described by Poiseuille's equation,

$$\eta = \pi \frac{P r^4 t}{8 V l} \quad \dots (2.4.1)$$

$\eta$  = coefficient of absolute viscosity,  $P$  = pressure causing flow,  $r$  = radius of tube,  $V$  = total volume of solution flowing,  $l$  = length of tube,  $t$  = time of flow.

For actual capillary flow it is necessary to correct the equation to,

$$\eta = \frac{\pi P r^4 t}{8 V(1 + cr)} - \frac{m V \rho}{8\pi(1 + cr)t} \quad \dots (2.4.2)$$

$m$  and  $c$  being constants.

Precise measurement of these constants is difficult<sup>41</sup>, hence it is usual to calibrate the viscometer by measuring flow times of liquids of known viscosity. For a kinematic viscometer, the equation reduces to the form,

$$\frac{\eta}{\rho''t} = A - \frac{B}{t^2} \quad \dots (2.4.3)$$

$A$  = constant,  $B$  = constant and  $\rho''$  = corrected density of the liquid considered (see later). As this equation is still not exact, it is more useful to use calibrating data to plot a large scale graph of  $\eta/\rho''t$  versus  $1/t^2$ <sup>42</sup>.

Drainage and surface tension effects can also lead to errors<sup>41,43</sup> but these may be reduced to negligible proportions if the viscometer has a large efflux volume and medium-bore capillary. Kelly<sup>42</sup> has discussed the experimental conditions necessary to achieve an accuracy of 0.1% in viscosity determinations. He noted that,

- (i) for recording to 0.1 sec, efflux time needs to be greater than 200 seconds. The flow times for carbon

tetrachloride at 35° and 45°C were 178.9 and 162.5 sec respectively; for benzene at 45°C, 191 sec. For those mentioned, and a few cases with dilute OMCTS mixtures, efflux times were below 200 sec. These exceptions were insufficient to warrant redesign of the viscometer.

- (ii) The temperature must be within  $\pm 0.015^\circ\text{C}$  of the required temperature. It was measured with  $10^\circ\text{C}$  range thermometers, which had been calibrated against a platinum resistance thermometer. Temperature control was by either a short-range contact thermometer ( $0 - 45^\circ\text{C}$ ), or a mercury-toluene regulator operating a Sunvic control relay. Control was normally within  $0.01^\circ\text{C}$  of desired temperature.
- (iii) The efflux volume must be constant to within 0.035 ml for a 25 ml viscometer. For the one used, the volume could be adjusted to within 0.02 ml of an etched mark.
- (iv) The density must be measured with an accuracy of 0.05% - this was easily achieved with the 27 ml pyknometers already described. As the liquid column is balanced at all times by an equal head of air, the density required in the equation given previously is,
- $$\rho'' = \rho - \rho_{\text{air}}$$
- (v) A deviation of 1.3 degrees in the alignment of the viscometer leads to an error of 0.05% in measurements. By using a

vertical cathetometer in two positions, approximately at right angles, the capillary could be adjusted to the vertical within 1 degree. The viscometer could be set to the fixed position repeatedly by sliding it and its holder into a fixed stand.

It should be noted that the discussion of the above points applies mainly to the measurement of viscosities of aqueous solutions. Expansion coefficients for non-aqueous liquids were larger than for water, therefore greater temperature control was necessary. Variations of the viscosity of the mixtures with temperature were sometimes greater, sometimes less than the variation with water - depending on the concentration.

### Calibration

The viscometer was calibrated with water at 20°, 25°, 35° and 40°C, and with benzene, carbon tetrachloride, 20% sucrose and 40% sucrose solutions at 25°C. Ideally, all the experimentally measured viscosities should fall within the curve given by these calibrating liquids, but the viscosities of a number of benzene and carbon tetrachloride mixtures with OMCTS at higher temperatures were outside the range. The error introduced by extrapolating from the steeply sloping portion of the calibration curve (Fig. 2.4.1) was estimated to be no more than 0.2%. It was felt these errors were no greater than those which would be introduced by using liquids of lower viscosity, as their viscosity values are not accurately known.

### Calibration liquids

(i) Water - The absolute viscosity of water at 20°C has been determined by Swindells, Coe and Godfrey<sup>44</sup>, who found that at 20°C it was equal to  $1.0019 \pm 0.0003$  centipoise compared with the previously accepted value of 1.005 centipoise. Values of the viscosity of water at other temperatures relative to the viscosity at 20°C have been tabulated by Coe and Godfrey<sup>45</sup> from the work of Cragoe.

$$\log \eta / \eta_{20} = \frac{(1.2348(20 - t) - 0.001467(t - 20)^2)}{(t + 96)} \quad \dots \quad (2.4.4)$$

The calculated values are summarised in Table 2.4.1.

(ii) Benzene - Timmermans<sup>32</sup> quotes three values for the viscosity of benzene at 25°C; viz, 0.596, 0.599 and 0.601 centipoise. Merker<sup>45</sup> quotes a value of 0.6031 centipoise which agrees with the water-calibration data. The National Bureau of Standards gives a value of 0.6010 centipoise.

(iii) Carbon tetrachloride - The viscosity of this substance quoted by Timmermans<sup>32</sup>, 0.8876 centipoise, appears to be in doubt. Kelly<sup>42</sup> has suggested the Thorpe and Roger value<sup>47</sup>, corrected for the new viscosity of water, 0.901 centipoise.

(iv) Sucrose solutions - Twice-recrystallised loaf sugar (Colonial Sugar Refining Co.) was dried in a vacuum oven at 80°C. From this stock, 20% and 40% by weight (in vacuo) solutions were prepared with deionised distilled water. The inevitable suspended particles were removed as previously described. The viscosities of sucrose solutions

TABLE 2.4.1

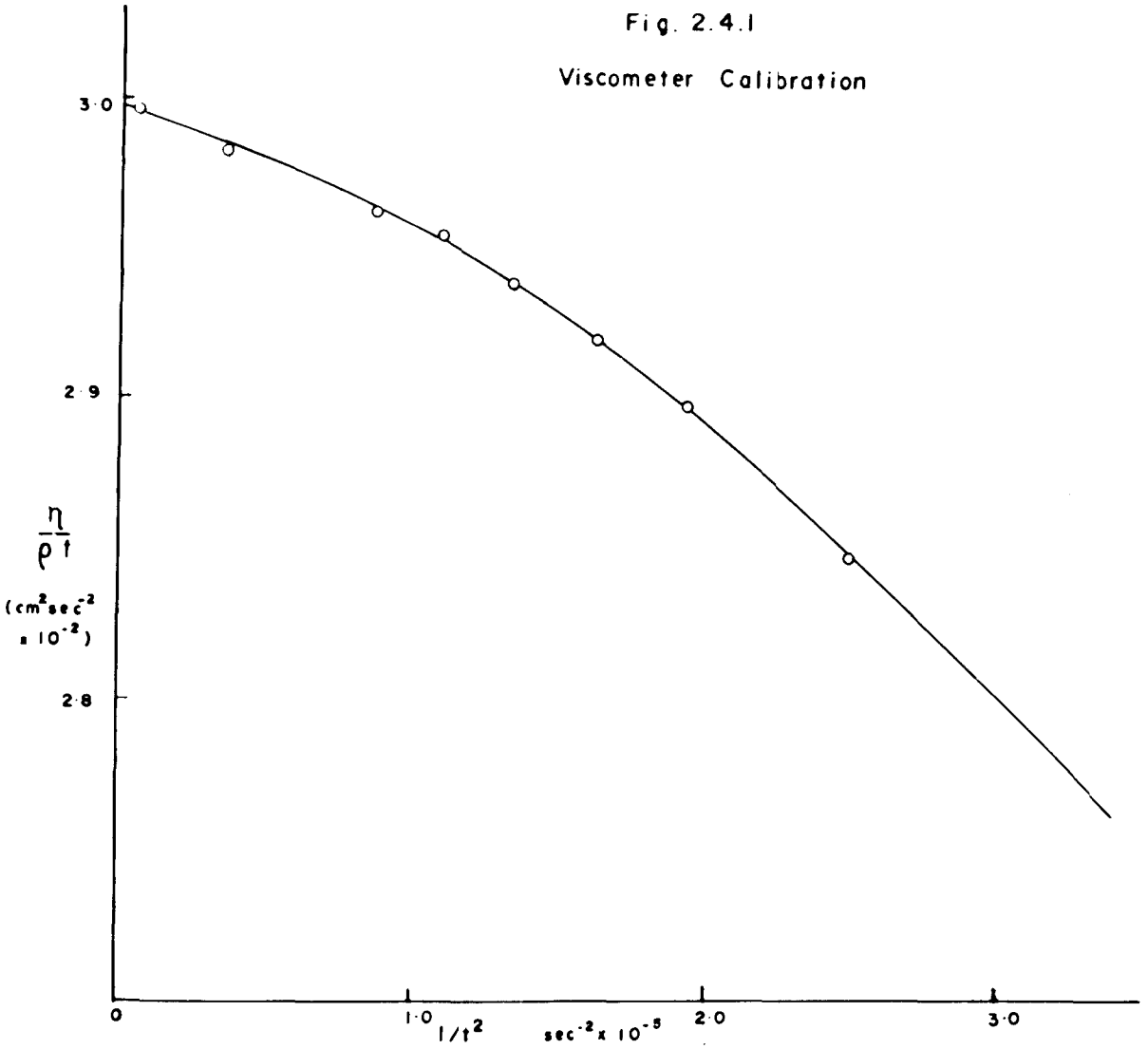
System	Viscosity $\eta$ (cp)	Density $\rho$ (g/ml)	Time $t$ (sec)	$\frac{\eta}{\rho t}$ ( $\text{cm}^2 \text{sec}^{-2} \times 10^2$ )	$1/t^2 \times 10^5$ ( $\text{sec}^{-2}$ )
$\text{CCl}_4$ - 25°C	0.901	1.58448	199.8	2.848	2.505
$\text{C}_6\text{H}_6$ - 25°C	0.6031	0.87336	237.4	2.909	1.774
$\text{H}_2\text{O}$ - 40°C	0.6531	0.99224	227.4	2.898	1.934
$\text{H}_2\text{O}$ - 35°C	0.7194	0.99406	248.1	2.920	1.625
$\text{H}_2\text{O}$ - 30°C	0.7976	0.99567	272.8	2.939	1.344
$\text{H}_2\text{O}$ - 25°C	0.8903	0.99707	302.6	2.955	1.092
$\text{H}_2\text{O}$ - 20°C	1.002	0.99823	339.2	2.962	0.871
Sucrose 20%					
- 25°C	1.695	1.0794	527.4	2.981	0.359
Sucrose 40%					
- 25°C	5.164	1.1745	1468.5	2.997	0.046

(corrected for the more recently accepted values of viscosity for water) were taken from Kelly's thesis<sup>42</sup>.

#### Experimental techniques

All solutions, except 20% and 40% sucrose, were filtered through a No.4 porosity filter immediately before use. The cleaned and dried viscometer, mounted in the bath, was filled by a long-needled syringe. After equilibration for thirty minutes, and adjustment of the level to the etched mark, the liquid was transferred to the upper bulb by air pressure and the time taken for the meniscus to travel between a further two etched

Fig. 2.4.1  
Viscometer Calibration



marks was recorded with a 30 second sweep stop-watch. Three measurements were made for each solution and an agreement within 0.1 second was considered satisfactory. For measurement of viscosity of mixtures at 18°, 35° and 45°C, a bulk solution of 100 mls was prepared and a 25 ml. aliquot was then introduced into the viscometer with the bath temperature initially at 18°C. After determining the efflux times, the solution was removed and its density measured at 25°C.

From this density reading, the concentration and density of the mixture at 18°C were calculated. The above procedure was repeated for viscosities at 35° and 45°C, a density measurement still being taken at 25°C in each case. The error produced by assuming a constant volume of mixing, over the temperature range, was negligible. Viscosities at 25°C were measured in separate experiments.

## 2.5 DIFFUSION - DIAPHRAGM CELL

### Introduction

The diaphragm cell measurements formed only a minor part of the diffusion study. The theory and operation of this cell has been adequately reviewed by Robinson and Stokes<sup>1</sup>, and more recently by Tyrrell<sup>48</sup>.

The diaphragm diffusion cell is an example of steady state diffusion giving relative diffusion coefficients. Diffusion takes place through a horizontal sintered-glass diaphragm separating two solutions

differing in concentration. The original diaphragm cell, introduced by Northrop and Anson<sup>49</sup> operated with the more concentrated solution in the top compartment. This arrangement promotes mixing by the diffusion process but there is the possibility of the denser solution streaming through the diaphragm. The cells used in this work have been described by Stokes<sup>50</sup>. The two surfaces of the diaphragm were swept by magnetically-operated stirrers and, in order to avoid streaming, the denser solution was placed in the lower compartment.

#### Comparison of the Diaphragm Cell with the Gouy Diffusiometer

The direct result calculated from the diaphragm diffusion cell is not the true diffusion coefficient - it is the diaphragm cell integral diffusion coefficient,  $\bar{D}$ , defined by,

$$\bar{D} = \frac{1}{\beta t} \ln \left( \frac{c_1 - c_2}{c_3 - c_4} \right) \quad \dots (2.5.1)$$

where  $\beta$  = cell constant,  $c_1$  and  $c_2$  are initial concentrations and  $c_3$  and  $c_4$  are concentrations in the two compartments at time  $t$ .

This diffusion coefficient is a double average of the differential diffusion coefficient,  $D$ . These two coefficients are related by the equation,

$$\bar{D} = \frac{1}{c_{m'} - c_{m''}} \int_{c_{m''}}^{c_{m'}} D \, dc \quad \dots (2.5.2)$$

where  $c_{m'} = \frac{c_1 + c_3}{2}$  and  $c_{m''} = \frac{c_2 + c_4}{2}$

The situation is less complex if the limiting diffusion coefficient

is known, as values of  $D$  may be determined from  $\bar{D}$  by successive graphical approximations. For electrolyte solutions, the limiting value may be determined from the Nernst equation. For other systems, it is necessary to express  $D$  as an arbitrary function of concentration, with the coefficients adjustable to fit observed  $\bar{D}$  values. When the diffusion coefficient varies rapidly with concentration, the problem of calculating  $D$  from  $\bar{D}$  is accentuated.

Further doubt exists regarding the use of the cell constant,  $\beta$ , for non-aqueous mixtures, since this constant is usually determined by diffusing 0.5M KCl into water. Mills<sup>51</sup> has shown that the limiting value obtained for the diffusion of diphenyl into benzene, from diaphragm cells, agrees with more absolute data<sup>23</sup>. However, it has not been shown that diaphragm cell results agree with absolute methods over the whole range of concentration.

To check this latter point, diphenyl was diffused into benzene in a diaphragm cell, and the results compared with the Gouy diffusimeter results of Sandquist and Lyons<sup>23</sup>. Agreement within 0.7% at an average concentration of 0.612M indicated that the calibration procedure, to be described, could be assumed to hold for diffusion measurements in non-aqueous media.

Diaphragm cells have the further disadvantage in that it is necessary to measure concentration differences accurately. For non-aqueous mixtures, measurement of the density is the most convenient

method of establishing the concentration and accuracy is then limited by the density difference of the two components. For OMCTS-carbon tetrachloride mixtures the density difference is sufficiently large, but for OMCTS-benzene mixtures the difference is much less, leading to less accurate results.

Owing to the disadvantages mentioned, and to the lack of knowledge of the variation of the diffusion coefficient with concentration, it was felt that the sole use of diaphragm cells was risky and unwarranted. In fact, the now-known variation in the diffusion coefficient with concentration for the benzene-OMCTS system would have been very difficult to calculate from the diaphragm integral diffusion coefficients. In order to establish the reliability of the diaphragm cell method a few measurements were made with the diaphragm cell on the OMCTS-carbon tetrachloride system.

#### Calibration of Diaphragm Cell

If the volume of a diaphragm cell consists of,

- (i) lower compartment volume  $V_1$
- (ii) upper compartment volume  $V_2$  and
- (iii) a diaphragm, volume  $V_3$ , in which the pores have effective cross-sectional area  $A$  and effective diffusion length  $l$ ,  
then the constant of the diaphragm cell is defined as,

$$\beta = \frac{A}{l} \left( \frac{1}{V_1} + \frac{1}{V_2} \right) \quad \dots \quad (2.5.3)$$

As the measurement of ratio  $A/l$  is difficult, it is more convenient to determine the cell constant by calibration with a solution

whose diaphragm cell integral diffusion coefficient is known, or can be calculated.

Those cells used were calibrated, as suggested by Stokes, by allowing approximately 0.5 N KCl to diffuse into water. The final concentrations,  $c_3$  (lower compartment) and  $c_4$  (upper compartment) were determined conductimetrically, following weight dilution. Conductivity data for potassium chloride was taken from the data of Shedlovsky<sup>52</sup> and Chambers<sup>53</sup>.

A Jones-Dike conductivity bridge was used to measure the conductance at 25°C in an oil-bath controlled to  $\pm 0.001^\circ\text{C}$ . Conductivity cells and ancillary apparatus have been described previously<sup>36</sup>,

For calibration runs the initial concentration in the upper compartment ( $c_2$ ) was zero and the concentration in the lower ( $c_1$ ) was determined from the conservation equation,

$$\left(V_1 + \frac{V_3}{2}\right)c_1 + \left(V_2 + \frac{V_3}{2}\right)c_2 = \left(V_1 + \frac{V_3}{2}\right)c_3 + \left(V_2 + \frac{V_3}{2}\right)c_4 \quad \dots (2.5.4)$$

The integral diffusion coefficients used in the calculations were taken from the tabulation by Stokes<sup>54</sup>.

### Results from calibrations.

The diaphragm cell constant,  $\beta$ , for each of the cells (designated by X, U, G and A) is summarised in Table 2.5.1. Volumes of the upper compartment, the lower compartment and the diaphragm ( $V_3$ ), are also included.

TABLE 2.5.1.

	<u>Cell X</u>	<u>Cell U</u>	<u>Cell G</u>	<u>Cell A</u>
$\beta$ initial	2.255	1.515	3.258	3.442
$\beta$ final	2.256	1.515	3.256	3.455
$V_1$ (ml )	57.736	59.135	55.93	58.11
$V_2$ (ml )	67.825	68.868	53.72	52.26
$V_3$ (ml )	0.508	0.232	0.56	0.63

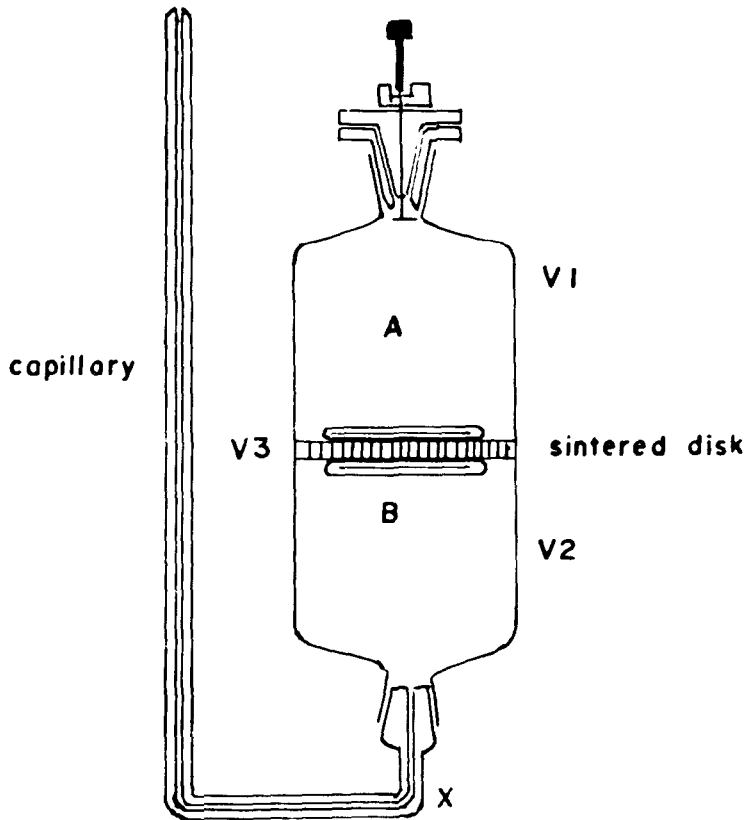
The initial and final cell constants agreed, except for the slight difference with cell A. This was to be expected as only a few runs were made with the cells.

#### Experimental techniques

Measurements were made on two systems:- OMCTS-carbon tetrachloride and benzene-diphenyl.

As carbon tetrachloride was denser than any of its mixtures, it was found necessary to invert the cell from its calibrating position. To allow for minor volume changes and evaporation, the lower plug was connected to a long bent capillary opening to the atmosphere (Fig. 2.5.1). For calibration, the capillary was broken at X and the cell inverted. It was felt that the volume of liquid in the capillary could not be considered as part of the diffusing solution. The upper compartment was fitted with a B10 teflon plug designed to eliminate dead space<sup>55</sup>. One of these stoppers was kindly supplied by Dr. R. Mills of the Australian

Fig. 2.5.1  
Diaphragm Cell



National University.

Owing to large density differences between the aqueous calibrating solution and some of the OMCTS-carbon tetrachloride mixtures, it was found necessary to use different stirrers; those which sank in the latter mixtures, inevitably pulverised the diaphragm when used with the aqueous KCl solutions. The replacement stirrers had volumes approximately equal to those of the original thus avoiding changes in the cell constant.

The diffusion cells were suspended by holders in a glass-fronted water bath. The bath was maintained at  $25.000 \pm 0.003^\circ\text{C}$  by a mercury-toluene regulator<sup>56</sup> controlling a 250 watt lamp through a Sunvic control relay. The horseshoe magnet stirrers were rotated (at 60 revs/min ) by a series of pulleys connected to the motor driving the paddle stirrer.

Before filling a diffusion cell, the solution and solvent were filtered through a No.4 porosity filter and degassed. After filling compartment A (see Fig. 2.5.1) and fitting the teflon stopper, the cell was placed with compartment A lowest, into the thermostatted water bath. On equilibrating for 25 minutes, the diaphragm was degassed by partial evacuation, carbon tetrachloride was added to the upper compartment and after stoppering, the cell was inverted.

At the end of the equilibration period (5 hours) the cell was inverted, and compartment B was rinsed a number of times with solvent before finally filling the cell and inverting. The starting time was taken at the final filling. At the completion of the run, the cell was

again inverted and a sample of solution withdrawn from compartment B by syringe. Likewise, a sample was taken from compartment A. The densities of the samples were taken at 25°C.

## 2.6 DIFFUSION - GOUY DIFFUSIOMETER

### Introduction

The majority of the diffusion coefficients recorded at 25°C, and all diffusion coefficients recorded at 18°, 35° and 45°C were determined with a Gouy diffusiometer. This apparatus measures free diffusion, where mutual diffusion occurs across an initially sharp boundary which exists between two solutions, or solution and solvent. For this experimental arrangement, the diffusion coefficient is defined by,

$$\frac{\partial c}{\partial t} = \frac{\partial}{\partial x} \left( D \frac{\partial c}{\partial x} \right) \quad \dots (2.6.1)$$

This differential equation has no general solution. However, by arranging the experimental conditions so that the diffusion coefficient is constant over the concentration range studied, then,

$$\frac{\partial c}{\partial t} = D \frac{\partial^2 c}{\partial x^2} \quad \dots (2.6.2)$$

When using a diffusion column, it is necessary to confine attention to the earlier stages of the diffusion process. Alternatively, the column must be sufficiently long in order that the concentration at the ends of the column remains invariant during an experiment. For this diffusion column,

$$\frac{\partial c}{\partial x} = \frac{1}{2} \Delta c (\pi Dt)^{-\frac{1}{2}} e^{-x^2/4Dt} \quad \dots (2.6.3)$$

where  $\Delta c$  = concentration difference between two uniform solutions  $c_1$  and  $c_2$ ,  $x$  = distance from original boundary,  $t$  = time elapsed since formation of boundary.

If a knowledge of  $\partial c/\partial x$  exists at any time  $t$ , the diffusion coefficient,  $D$ , may be calculated. Determining this concentration gradient directly in a diffusing column is difficult. Therefore, it is convenient, and certainly more accurate, to determine the refractive index gradient. If refractive index,  $n$ , is assumed to be a linear function of concentration over the small concentration difference under consideration, equation (2.6.3) becomes,

$$\frac{\partial n}{\partial x} = \frac{1}{2} \Delta n (\pi Dt)^{-\frac{1}{2}} e^{-x^2/4Dt} \quad \dots (2.6.4)$$

This equation assumes a pure Gaussian distribution about the position of the initial boundary. Skewed Gaussian curves may be observed in binary systems where either the diffusion coefficient or the refractive index increment varies with concentration. For the former case, it is necessary to assume some relationship between the diffusion coefficient and concentration. One proposal is that of Fujita<sup>57</sup>, who considered  $D$  as a function of  $1/c$ . Gosting and Fujita<sup>58</sup> considered a Taylor expansion series for the variation of refractive index with concentration. Longworth<sup>59</sup> has pointed out that in some systems the variation of  $D$  with concentration is balanced by the refractive index increment variation, and a symmetrical Gaussian curve results.

The refractive index gradient may be measured by a number of optical means, including the Gouy interference method. Using the optical system depicted in Fig. 2.6.1 Gouy interference fringes may be observed as diffusion occurs from an initially sharp boundary.

A theory, based on geometric optics, to explain Gouy fringes was first presented by Gosting et al.<sup>60</sup> and Coulson et al.<sup>61</sup>. Gosting and Onsager<sup>62</sup> have shown that the geometric optical reasoning is not adequate and their approach, based on wave optics, gives a better representation of the fringe displacement.

#### Calculation of diffusion coefficients.

Information obtainable from a photograph of a set of Gouy fringes at a time  $t$  is (i) the displacement of the fringe minima above or below the optic axis ( $Y_J$ ) where  $J = 0, 1, 2 \dots$ ; numbering being from the fringe furthest from the optic axis, and (ii) the total number of fringes,  $J_m$ . This value includes the fractional fringe determined from the displaced Rayleigh fringe pattern.

The reduced height area ratio defined by,

$$D_a = \frac{(\Delta n)^2}{4\pi t (\partial n / \partial x)_{\max}^2} \quad \dots (2.6.5)$$

where  $(\partial n / \partial x)_{\max}$  is the maximum value of  $\partial n / \partial x$  at a time  $t$ , reduces to,

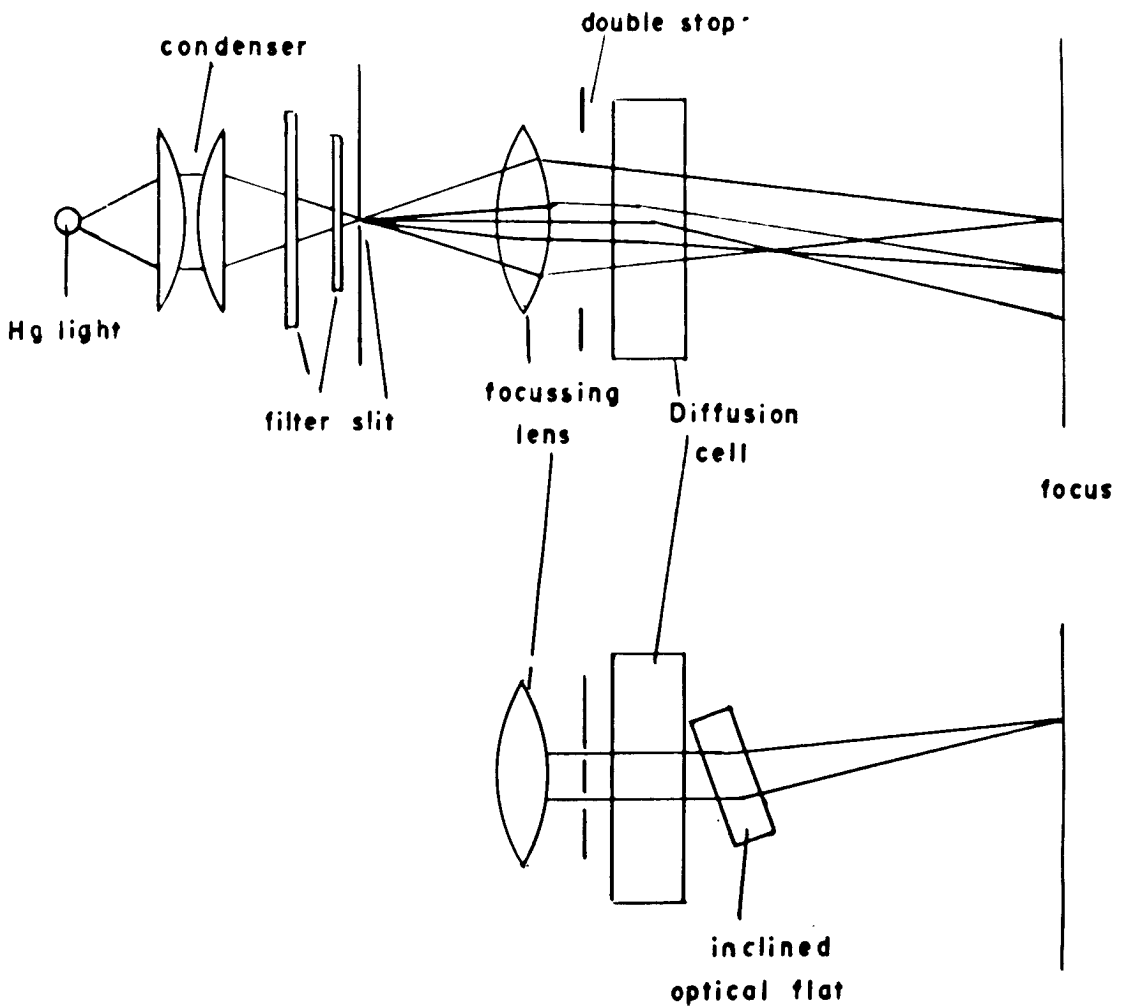
$$D_a = \frac{J_m^2}{t c_t^2} \frac{(b\lambda)^2}{4\pi} \quad \dots (2.6.6)$$

$\lambda$  = wavelength of the monochromatic light,  $b$  = optical lever arm

$c_t$  = maximum deflection of light at time  $t$ .

Fig. 2.6.1

Optical System - Gouy Diffusimeter



The optical lever arm is defined by  $b = \Sigma l/n$ ,  $l$  being the distance through each medium of refractive index  $n$  - thus  $b$  is the "optical" distance from the centre of the cell to the photographic plate. The value  $c_t$  is given by  $e^{Z^2} Y_J$ , where the function  $e^{Z^2}$  can be calculated from the tables of  $e^{Z^2}$  versus the reduced fringe number  $f(Z)$ ,

$$f(Z) = J + \frac{3}{4} + \dots / J_m \quad \dots \quad (2.6.7)$$

this function being derived from the refined wave optics theory<sup>62</sup>.  $J$  is the fringe number.

For a two component system where the refractive index shows a linear dependence on concentration, and the diffusion coefficient is independent of concentration, the reduced height area ratio,  $D_a$ , is equal to diffusion coefficient  $D$ .

#### Diffusimeter.

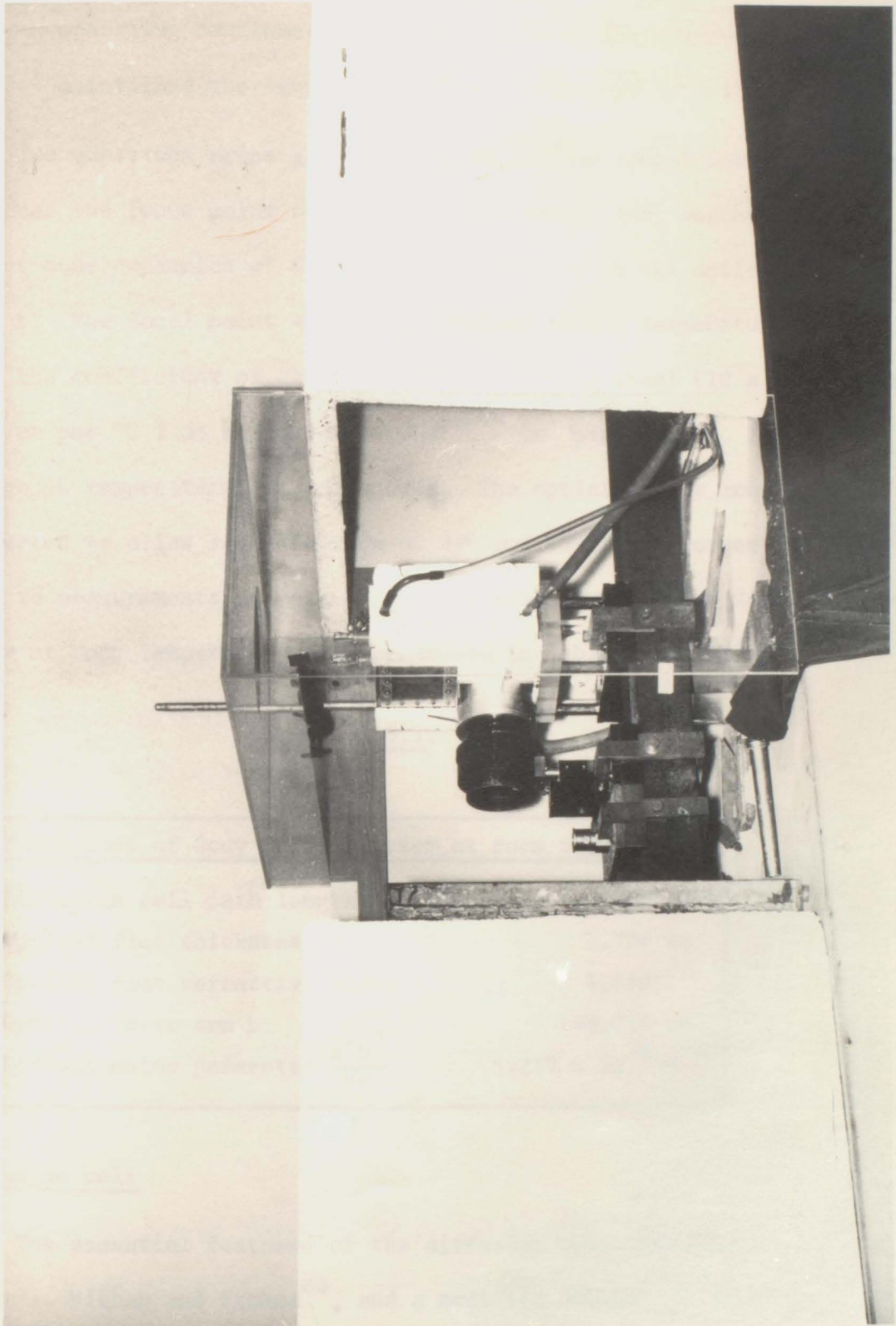
The Gouy apparatus used has been described in detail<sup>63</sup>. The optical arrangement was similar to that of Gosting<sup>60</sup>, while the diffusion cell itself was an enlarged version of the flowing junction type used by Coulson et al.<sup>61</sup>. The setting-up of the instrument has been described by Dunn<sup>64</sup>. The following points should be noted:

- (i) The slit, double stop, lens and the cell were aligned parallel by means of a cathetometer, rather than relying on the optical bench being parallel.
- (ii) The slit, of width approximately  $10\mu$ , was made by mechanically moving a new razor blade across a blackened

photographic plate. To maintain good control on slit width the razor was clamped on a suitably loaded jig, connected to the horizontal travel of a mill.

- (iii) The refractive index gradient for the benzene-OMCTS system was in the reverse direction to the density gradient resulting in a reversed Gouy pattern. The plateholder position had to be altered to another position, where checking of the operation of the diffusimeter with a sucrose solution was impossible, hence the optical lever arm distance,  $b$ , was checked after each movement.
- (iv) The focal point and optical lever arm were found to be unaltered (within experimental error) for the various solutions used in the diffusion cell.
- (v) At 35° and 45°C, the whole optical bench was placed in a thermostatted jacket (Fig. 2.6.2). The jacket was made in three parts: one part covered from the light source to focussing lens, another from the diffusion cell to the photographic plate. The third portion was a clear Perspex box, containing openings for a hand glove and thermometer, and it covered the central section containing the diffusion cell and the double stop. The first two parts were made from 1½" thick polystyrene foam sheeting. A fan and fan heater,

Fig. 2.6.2



operating continually through a contact thermometer, maintained the temperature of the enclosure to  $\pm 1^\circ\text{C}$ .

Two questions arise when working at unusual temperatures. Firstly, how does the focus point change with temperature and, secondly, what effect does expansion of the optical bench have on the optical lever arm,  $b$ ? The focal point was found constant at all temperatures, and from the coefficient of linear expansion of mild steel ( $10 \times 10^{-6}$  cm per unit cm per  $^\circ\text{C}$ ) an expansion of  $2 \times 10^{-4}$  cm per unit cm for a  $20^\circ\text{C}$  change in temperature was calculated. The optical lever arm,  $b$ , was corrected to allow for expansion at  $35^\circ$  and  $45^\circ\text{C}$ . No correction was made to measurements made at  $18^\circ\text{C}$ . The dimensions of the Gouy diffusio- meter at room temperature are summarised in Table 2.6.1.

TABLE 2.6.1.

<u>Dimensions of Gouy Diffusimeter at room temperature</u>	
Diffusion cell path length	2.250 cm
Optical flat thickness	1.726 cm
Optical flat refractive index	1.510
Optical lever arm $b$	148.319 cm
Diffusimeter parameter $\frac{\lambda^2 b^2}{4\pi}$	$5.217 \times 10^{-6} \text{ cm}^4$

### Diffusion cell

The essential features of the diffusion cell have been described by Hall, Wishaw and Stokes<sup>63</sup>, and a modified version of the cell<sup>64</sup> was

available at the commencement of this work. As this cell was fabricated from perspex, it was obviously unsuitable for working with benzene and carbon tetrachloride; hence a new cell was constructed from stainless steel. Further modifications to cell design included a new method for constructing the flowing junction, a greaseless overflow valve and the use of glass reservoirs. Further, the number of parts used in making the cell was reduced, without loss in solidity. The cell is shown in Fig. 2.6.3.

All components of the cell were milled and lapped, from stainless steel, by Mr. C.W. Tuxford of the workshop staff. The hand-lapping of the surfaces was of such a standard that when the eight parts were pinned together, without the use of cement or glue, no leakages occurred at any joints, when pressures of up to  $\frac{1}{4}$  atmosphere were applied. The flowing junction was made by milling a section 0.0015 inches deep across the top section of F. The junction was connected to an overflow area and control of the flow rate was maintained by a valve (Fig. 2.6.3). This valve was closed on forcing a teflon plunger into a tapered cone by turning a knurled screw. Leakage around the threaded screw was prevented by a Neoprene O-ring. Application of several atmospheres pressure to the valve indicated an absence of leakage.

The tap design had a number of advantages.

(i) It was possible to seat the tap within the constant

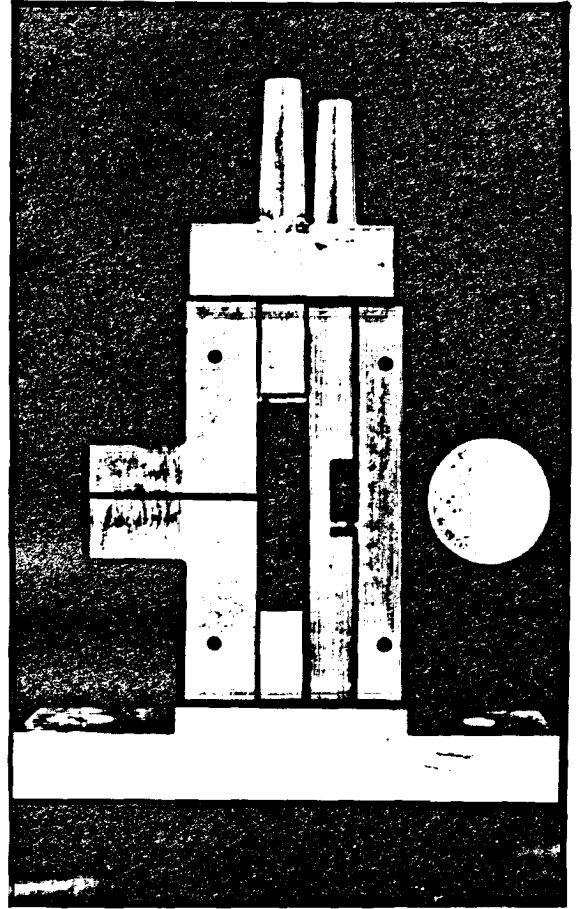
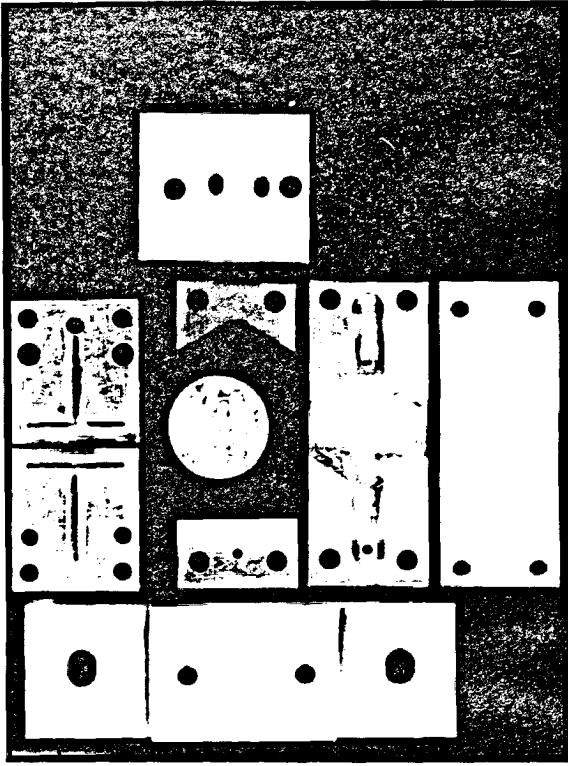
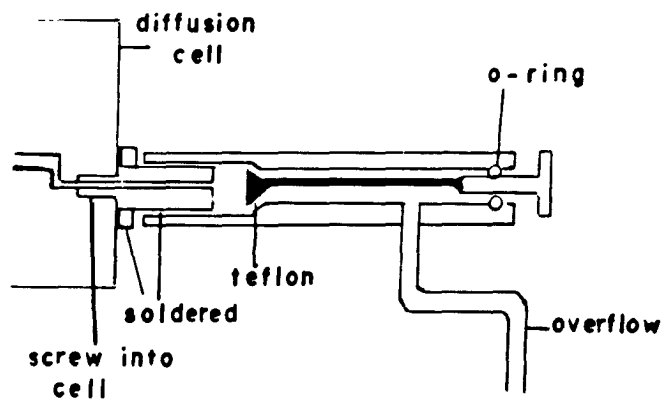


Fig. 2.6.3

Fig. 2.6.3b Valve



temperature enclosure.

- (ii) As the tap operated in the direction of overflow, closure did not force solution back through the slit.
- (iii) Good control of the flow rate could be maintained at all times during the sharpening procedure.

The glass solution reservoirs were connected to the diffusion cell by B7 tapered joints fitted with teflon sleeves. They were held in position by two phosphor-bronze springs. Initially, the compartment volumes were approximately 60 ml, but these were later changed to 100 ml capacity. Evaporation losses were reduced by placing saturators on top of the solution reservoirs. A tapered teflon plug connected to a brass rod<sup>64</sup> replaced the original gate valve.

The optical flats were held in position by frames which screwed onto the cell. With no sealing between optical flats and the lapped walls of the cell, slight leakages were noted. It was found expedient to spread a small amount of dispersed teflon (from a pressurised spray-can) around the area immediately before positioning the optical flats. Finally, the area was given a good coating of high-melting Kel F grease.

Initially, the cell was surrounded by a Perspex water bath. This was changed later to a brass reservoir of simpler construction. Water from a thermostatted tank, under the concrete bench, was pumped through this upper reservoir. The pump also circulated the water in the lower tank.

The temperature-control system was similar to that used in measuring viscosities. Control at all temperatures was of the order of  $\pm 0.008^\circ\text{C}$ . It should be noted that greater temperature control is necessary for non-aqueous solutions than for aqueous solutions, owing to the former having a greater variation of density and refractive index with temperature.

### Techniques.

Correct operation of the diffusimeter was established by comparing the diffusion coefficients obtained by diffusing 0.35N KCl into 0.15N KCl, and diffusing sucrose into water, with those reported by Gosting<sup>65</sup> and Gosting and Morris<sup>66</sup>, respectively. Agreement within 0.1% was considered satisfactory.

The cell-filling procedure, the boundary sharpening and diffusion run have been described previously<sup>64</sup>. A brief summary is now given.

- (i) Reservoir 2, the reference channel and the diffusion channel were filled with the denser solution. After positioning the teflon plug in Reservoir 1, the less dense solution was added. Finally, small saturators were placed on the B10 sockets above each reservoir.
- (ii) The solution was equilibrated for 25 minutes before forming the boundary. During this time three exposures were taken with the double stop in position and from these the position of the optic axis was determined with respect to the reference pattern.

- (iii) After 30 minutes of boundary sharpening and further equilibration, the Rayleigh fringe displacement pattern was photographed.
- (iv) Six exposures were taken at approximately equal intervals of  $1/t$ .
- (v) Measurements at 18°, 35° and 45°C were made with the same solutions. At the end of a run at one temperature, the boundary was re-formed, temperature altered and the cell contents re-equilibrated before another run was commenced. Equilibration and sharpening were followed by observation of the image at the plate focus point.
- (vi) After completion of work at 45°C, the tapered plug was repositioned, the contents of each compartment were removed using syringes and concentrations were determined from density measurements at 25°C. Concentrations in the two compartments were measured at the completion of, rather than prior to an experiment, as slight concentration changes due to evaporation inevitably occurred when rinsing the cell. The 25°C diffusion results were obtained from separate experiments using similar procedures.

Owing to the small supply of OMCTS available, experiments were started at high OMCTS concentrations and, upon completion of one experiment, solutions were treated appropriately to provide two less-concentrated solutions. By this continual dilution process, the whole concentration range could be covered. Diffusion measurements were made on a number

of check solutions to establish the correctness of the procedure. Sandquist and Lyons<sup>23</sup> have noted that the presence of impurities has little effect on the diffusion coefficient - therefore, any contamination introduced by this dilution process would not be likely to affect diffusion results.

The plates were measured to  $\pm 2\mu$  on a Hilger travelling microscope and calculations were made along the lines suggested by Gosting<sup>65</sup>. Detailed examples of the calculations have been given by Dunn<sup>64</sup> and Kelly<sup>42</sup>. Extrapolation of the calculated values of  $D_a$  against  $1/t$  to  $1/t = 0$  gave the diffusion coefficient. Extrapolation was necessary because of the inability to form a perfect boundary at zero time. As previously noted by Dunn<sup>64</sup> and Kelly<sup>42</sup>, a disparity existed between the fringe number as given by the sum of the integral part of  $J_m$  (obtained by counting fringes) and the fractional part,  $\alpha$ , (obtained from the displaced Rayleigh fringe pattern) and the value required to give constancy in  $e^{z^2} Y_J$ . Accurate positioning of the double stop by a cathetometer (suggested by Kelly) has not removed this discrepancy.

## 2.7 ACTIVITY COEFFICIENTS

### Introduction

The activity coefficient of one of the components in a non-aqueous binary mixture may be determined by the following methods:

- (i) Gas-liquid chromatography

- (ii) Vacuum balance
- (iii) Ebulliometer
- (iv) Vapour pressure recirculating still
- (v) Freezing point depression
- (vi) Static vapour pressure measurements.

A discussion on the relative advantages and disadvantages of each method follows.

#### (i) Gas-liquid chromatography

The activity coefficient of a volatile component of a two component mixture may be determined at infinite dilution by gas chromatographic techniques<sup>67,68</sup>. In an experiment, the volatile component is passed over the involatile, which is held in an inert stationary phase.

From a knowledge of the variation of the initial and peak retention volumes, peak heights and peak widths<sup>68</sup> with the sample size of the volatile component and the flow rate, the peak retention volume appropriate to an ideal column,  $V_R^0$ , may be calculated. An ideal column is one in which,

- (a) equilibrium is maintained between vapour and liquid,
- (b) Henry's law is obeyed and
- (c) the pressure drop across the column is zero.

Everett<sup>69</sup> has shown how the activity coefficient at infinite dilution may be calculated from this peak retention volume,  $V_R^0$ . Theoretically the correct methods for determining activity coefficients over a concentration range have been established<sup>69</sup> but, in practice, it

is doubtful if any real column can be made to behave in exact accordance with theoretical models.

(ii) Vacuum balance

A vacuum balance experiment involves the measurement of the equilibrium composition of a mixture containing a fixed amount of a non-volatile component when exposed to the vapour of a volatile component at a known vapour pressure and temperature. In effect the absorption isotherm is determined. Experimentally, the non-volatile component is held in a vacuum balance and the change in weight is observed after a known amount of volatile component is added to the system<sup>70,71,72</sup>. This type of apparatus may be used to cover the whole concentration and temperature range in one run. However, the method is limited to the case where one component is effectively involatile. OMCTS has a vapour pressure of 1.00 mm Hg at 25°C and 9.75 mm Hg at 60°C so that the vacuum balance type of apparatus would not have been suitable unless it had been greatly modified.

(iii) Ebulliometer

Activity coefficients may be determined from the elevation in boiling point of a volatile component upon addition of an involatile component. This method was not suitable, as measurements are usually made at constant pressure. Furthermore, difficulties arise when working at pressures below atmospheric.

(iv) Vapour pressure still

Recirculating vapour pressure stills have been widely used for measurement of liquid-vapour equilibrium<sup>73,74</sup>. In this apparatus, there is a danger of establishing a false state of equilibrium by either enrichment of the vapour by partial condensation or by impoverishing the vapour by entrainment of liquid droplets. At low temperatures and pressures further problems arise, owing to the presence of radiant heat from the heaters<sup>75</sup>.

(v) Freezing point depression

Activity coefficients may be obtained from freezing point depressions. The method is useful, though limited. The error in activity coefficients determined by vapour pressure techniques increases with decreasing temperature because of the lower vapour pressures. At the freezing point vapour pressures are usually quite small. Activity coefficients from freezing point depressions give a guide to the form of extrapolation needed to obtain results at temperatures intermediate between the freezing temperature and the temperature where the various vapour pressure techniques give accurate results.

(vi) Static vapour pressure measurements

Scatchard has put forward the case for static vapour measurements. He states,<sup>76</sup> "In the course of developing equilibrium stills we have become more and more impressed by the intrinsic disadvantages and uncertainties of this method. The static method has the advantages

that it measures true equilibrium, it is more precise and it can be used to much smaller pressures. It has the disadvantages that it cannot be used with components which decompose, and that the vapour composition cannot be measured but must be calculated".

Precision static vapour pressure measurements make stringent demands as regards determination of composition of liquid mixtures, control and measurement of temperatures and the thorough degassing of the liquids. Ideas for the static vapour pressure apparatus used were taken from the following studies: Baxendale, Enüstun and Stern on benzene-diphenyl,<sup>77</sup> Everett and Penney on benzene-diphenyl, benzene-diphenylmethane and benzene-dibenzyl,<sup>27</sup> and McGlashan and Williamson on n-hexane-n-hexadecane<sup>26</sup>. It is believed that the accuracy obtainable from the apparatus to be described approaches that obtained in the abovementioned studies, but in saying this, it is necessary to acknowledge the debt owing for ideas contained within these earlier studies.

In the static method, total vapour pressure is measured as a function of total composition. The liquid and vapour composition may be determined from a knowledge of the volumes occupied by the vapour and liquid and the appropriate use of the Gibbs-Duhem equation<sup>78</sup>. A brief outline of the calculation follows, together with apparatus details. Appendix I gives further details of the calculations.

#### Calculation of activity coefficients

The activity coefficient of the volatile component (component 2) is given by

$$\ln f_2 = \ln\left(\frac{p_2}{p_2^0 x_2}\right) + \frac{(B_{22} - V_2^0)(p - p_2^0)}{RT} - \frac{B_{22}^2(p^2 - p_2^{02})}{2(RT)^2} + \frac{(V_2^0 - V_2)(p - p^*)}{RT} \quad \dots (2.7.1)$$

$p_2$  = vapour pressure of component 2 over mixture with total pressure  $p$

$p_2^0$  = vapour pressure of pure 2 at the same temperature ( $T^\circ A$ )

$B_{22}$  = second virial coefficient

$V_2^0$  = molar volume of pure 2

$V_2$  = partial molar volume of 2 at mole fraction  $x_2$

$p^*$  = arbitrary reference pressure.

Provided that  $p$  is less than one atmosphere,  $p^*$  is chosen to be less than one atmosphere and provided also that the partial molar volume does not vary excessively with concentration, the final term may be neglected. This equation assumes that the virial coefficient terms containing  $B_{21}$ ,  $B_{11}$ ,  $C_{222}$  and  $C_{221}$  etc. contribute a negligible amount to the correction for nonideality of the vapour phase. The third term may also be neglected.

From the masses of the components in the mixture, the total mole fraction of OMCTS, component 1, was calculated. Using this value an approximate vapour pressure of 1 was calculated, and subtraction from the total vapour pressure gave an approximate vapour pressure of component 2 - the volatile component. From a knowledge of the total volume available to the vapours and their approximate vapour pressures, the number of moles of each component in the gas phase was calculated. Subtraction from total moles gave the number of moles in the liquid

phase. This cycle of calculation was repeated until the vapour pressure of the volatile component was constant. This calculation assumes ideal behaviour for the less volatile component, a false assumption according to the Gibbs-Duhem equation,

$$x_1 \partial \ln f_1 / \partial x_2 + x_2 \partial \ln f_2 / \partial x_2 = 0 \quad \dots (2.7.2)$$

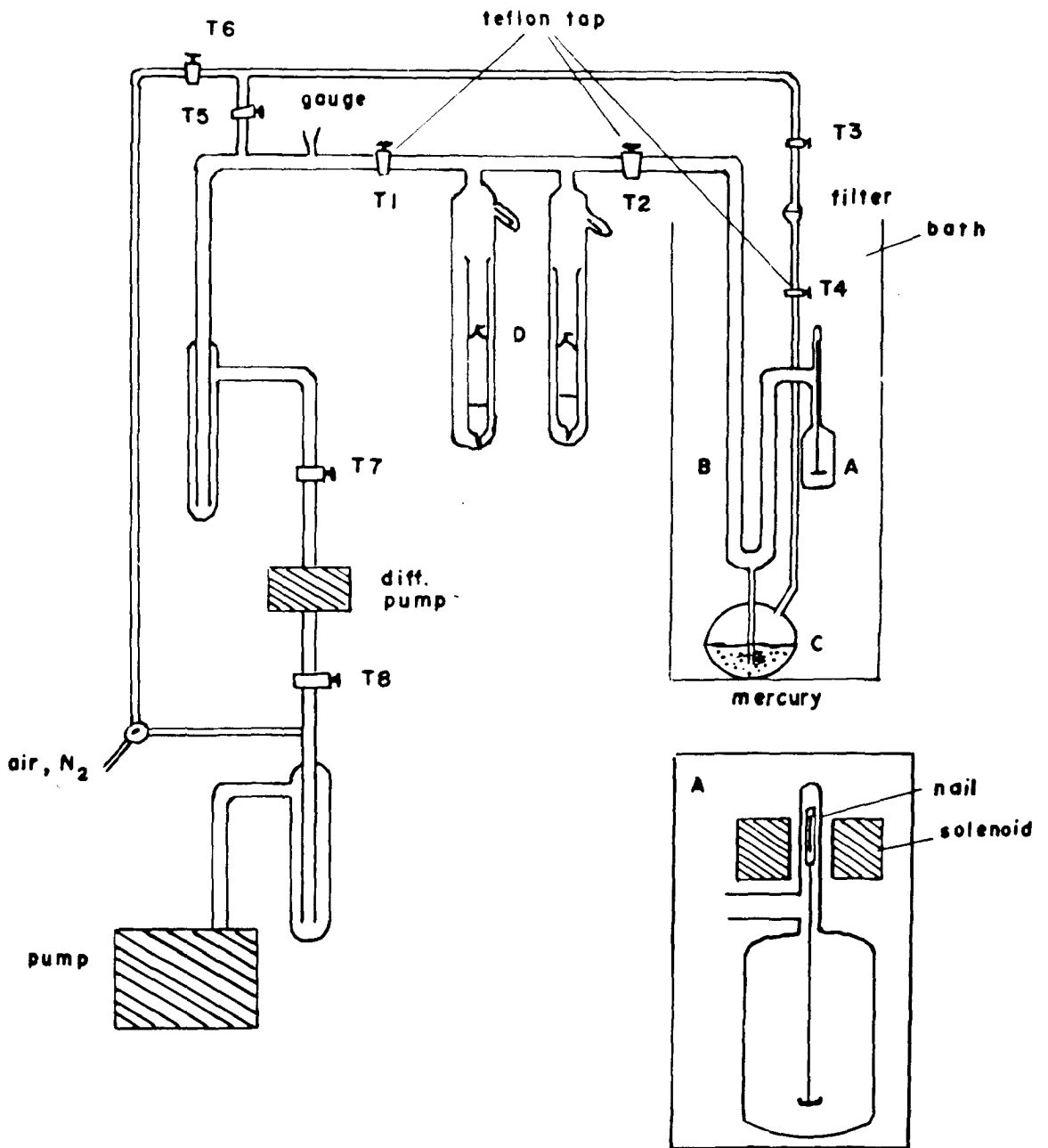
A refinement involves calculating the activity coefficient of component 1, at the required concentration, utilising the above equation, correcting for non-ideality and repeating the calculations until constancy again results.

#### Vapour pressure apparatus

A schematic diagram is given in Fig. 2.7.1. Total vapour pressure above the liquid in cell A was measured by the mercury manometer B. McGlashan<sup>26</sup> has pointed out advantages in measuring pressure directly, but he rejected this method on the grounds of constructional difficulties involved in producing a thermostat of sufficient height, while retaining good temperature control. The nulling type bellows manometers described<sup>76,27</sup> were rejected owing to disadvantages; viz, outgassing, change in zero point and susceptibility to vibration. The recently described stainless-steel capacitance manometer manufactured by Granville Phillips and the quartz spiral gauge manufactured by Texas Instruments appear to have overcome these difficulties. The use of a single manometer reduced considerably the number of measurements and operations required for a pressure observation, and inclusion

Fig. 2.7.1

Vapour Pressure Apparatus



within the thermostat eliminated the necessity of a second manometer thermostatted near room temperature.

The manometer was constructed from 10 mm. diameter precision bore "Veridia" tubing. Mercury was moved up or down the manometer by applying either air pressure or vacuum to the mercury reservoir via taps T6, T3 and T4. By suitable operation of the three taps, small adjustments to the height were readily achieved. A No.4 porosity filter placed between taps T3 and T4 produced a pressure gradient between these taps, enabling mercury to move up the column very slowly, eliminating the "back lash" normally associated with mercury moving in a column. Tap T4, a teflon tap immersed below the water level, was kept closed during a pressure measurement so that air pressure maintaining the mercury column was at constant temperature. A balancing air pressure, rather than a tap between the reservoir and mercury column, was used because of the difficulty in operating a tap at the bottom of the tall thermostat, especially at high temperatures. Calculation showed that a change of 0.01°C would have a negligible effect on the pressure in the balancing column - hence on the height of mercury in the manometer. Taps T1 and T2 were the teflon taps (Fisher and Porter) described previously. The ampoule holders, D, were sealed on between these two taps. The remaining part of the apparatus consisted of an Edwards Pirani gauge, liquid air trap, a metal mercury diffusion pump (Edwards type 1M1), a second liquid air trap and a backing pump (Metrovac). The vacuum system, with the exception of the backing pump and the second

liquid air trap, was mounted on a vertically movable frame. A photograph of the frame is shown in Fig. 2.7.2. The side of the frame immersed in the thermostat was constructed from brass and the other two from steel. Six plain brass bearings connected the frame to the three accurately parallel 1" diameter silver steel runners. To reduce the possibility of the frame sticking due to misalignment, bearings were loosely connected to the frame. The three runners were held in position by two half inch steel plates. The base plate was bolted to a concrete bench and the top plate held rigid by connections to the wall. The frame was moved up and down by a small trailer winch. The backing pump, placed on the floor to prevent vibration, was connected to the diffusion pump by a long piece of flexible rubber vacuum tubing.

The thermostat was a 110 litre copper tank (37 x 37 x 80 cm.) with two sides fitted with glass viewing windows 12 cm wide, running the full length of the bath. It was insulated on the sides and bottom by an inch layer of Canite and similar covers fitted over the glass windows. The top was covered with a plastic sheet when working at higher temperatures. The bath was stirred by three five inch diameter propellers distributed evenly along a vertical shaft situated in one corner of the bath. The stirrer was driven by a half horsepower motor situated on the concrete bench. The stirring rate was approximately 480 revs/min. Observation indicated no stagnant layers in the thermostat.

#### Temperature control

A specially designed mercury-toluene regulator was employed for

Fig. 2.7.2



temperature control. This regulator, operating through a Sunvic relay and a proportioning head, switched a 60 watt light bulb to provide the intermittent heating source. At temperatures above room temperature, a second heater was operated through a variac transformer. This auxiliary heater consisted of an 11 metre length of Pyrotanax heating cable wound evenly down a frame which was situated on one side of the bath. The voltage applied to this heater was adjusted in order that the "on" and "off" times for the intermittent heater were the same - about 10 seconds. The 400 ml capacity mercury-toluene regulator is shown schematically in Fig. 2.7.3. By using a large number of  $\frac{1}{4}$ " diameter copper "fingers", the response time of this regulator was very rapid and, by having the mercury reservoirs of a sufficient capacity (50 ml), the whole temperature range could be conveniently covered. A movement of  $1\frac{1}{2}$ " of mercury in the narrow-bore capillary corresponded to a temperature change of  $0.020^{\circ}\text{C}$ .

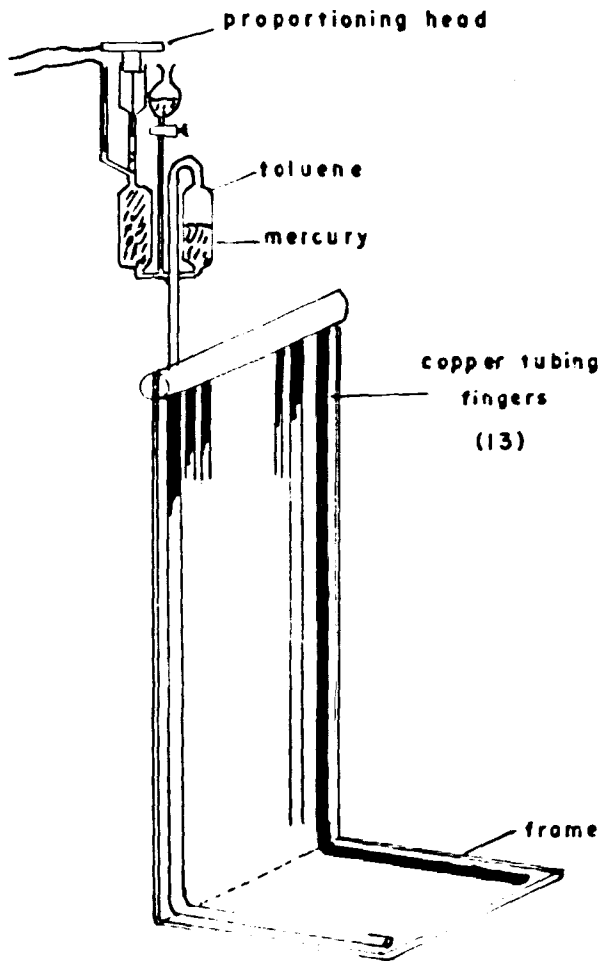
For the rapid heating required to raise the temperature to the next working temperature, three 1250 watt heaters were employed.

#### Temperature measurement

The thermostat temperature was measured with a Cambridge platinum resistance thermometer - number C552969. This thermometer had been calibrated in 1953 but its constructional details (width, depth etc.) were such that it could not be calibrated directly by the National Standards Laboratory. At the completion of this work, a calibrated

Fig. 2.7.3

Mercury Toluene Regulator



Leeds and Northrup standard platinum resistance thermometer (model number 167950), calibrated by the N.S.L. in 1966, became available and the two thermometers were found to agree within 0.002°C at 5°, 25° and 60°C.

The resistance of the thermometers was measured on a Cambridge Smith's difference bridge (L320720) using a Honeywell "Brown Electronic" null detector (model 104 W1). Using maximum sensitivity and 2 mA current through the bridge, a resistance change of 0.0001 ohm could be easily detected.

To ensure maximum reproducibility in measured resistances, the room was thermostatted near 20°C and the oil, surrounding the bridge resistances, was stirred. The ice used to establish the resistance at 0°C was prepared from deionized distilled water. Special care was taken to prevent contamination when crushing and transferring this ice. To eliminate the absorption of radiant heat from the intermittent heat source, the thermometer was placed in a copper jacket while in the thermostat. To provide adequate circulation around the thermometer, a number of holes were drilled in the side opposite the heating lamp.

The calibration figures for the Cambridge resistance thermometer are given below, viz,

$$\frac{R_{100}}{R_0} = 1.38989 ,$$

$$\frac{R_{444.6}}{R_0} = 2.6433$$

and

$$\frac{R_{-182.97}}{R_0} = 0.2480$$

Temperatures in degrees Centigrade were calculated from the Callendar equation,<sup>79</sup>

$$t = \frac{100(R_t - R_0)}{(R_{100} - R_0)} + \delta(t/100 - 1)t/100 \dots (2.7.3)$$

The constant  $\delta$  equal to  $1.509 \times 10^{-4} (\text{°C})^{-1}$  was calculated from the calibration results and the temperature,  $t^{\circ}\text{C}$ , was calculated by successive approximations.

It should be noted that the thermometer specifications were outside the range set in 1948 for "standard" platinum resistance thermometers<sup>80</sup> - a contributing factor to reasons given by the Standards Laboratory for their inability to calibrate the thermometer. The Leeds and Northrup thermometer, however, was within the required specifications.

A set of 32 thermometers by Emil, covering the range  $0^{\circ}\text{C} - 100^{\circ}\text{C}$  in  $6^{\circ}\text{C}$  overlapping intervals, was available. These were used for rough adjustment of temperature. They were not calibrated as a greater reproducibility of the temperature scale could be obtained by using the resistance thermometer for all serious temperature measurements.

Details of construction and operation of the Smith's difference bridge have been described elsewhere<sup>81,82</sup>.

### Pressure measurement

The manometer was made from 10 mm bore Veridia precision bore tubing. For a tube of this size, mercury shows a considerable capillary rise,<sup>83</sup> but this effect should cancel if the meniscus height for each mercury surface is the same. By careful control and by always

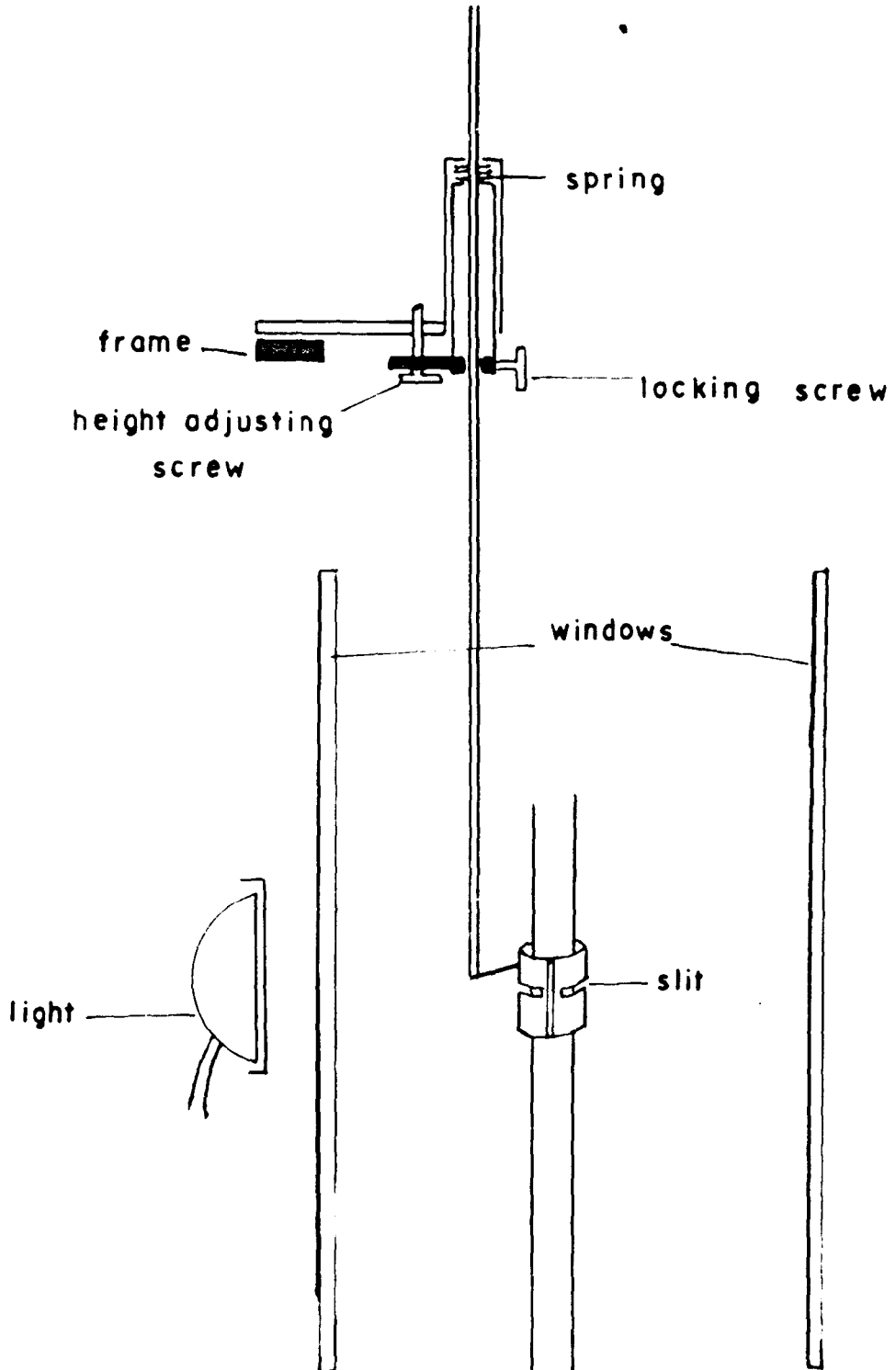
using a rising meniscus, the latter situation could be achieved - hence, errors arising from this phenomenon were considered less than 0.02 mm Hg. This effect could have been eliminated by using 20 mm constant-bore tubing but none was available when work commenced.

The meniscus was illuminated by a diffuse light source (a desk lamp covered with a white towel). Stray light in the vicinity of the meniscus was eliminated by fitting cylindrical brass shields around each manometer arm. Each shield had a 1 mm slit cut in the front and back. By adjusting the distance between the bottom of the slit and the mercury level to less than 0.25 mm, the meniscus position was found independent of the precise position of the brass shields<sup>26</sup>. The shield height could be adjusted from the top of the bath by a fine screw control (Fig. 2.7.4).

Mercury heights were measured with a Precision Tool and Instrument Co. 1 metre cathetometer (number 15477). It remained uncalibrated as no suitable scale was available. Previous experience<sup>26</sup> has shown these instruments accurate to  $\pm 0.01$  mm. The makers state that the brass scale was ruled at 20°C and, as the room was thermostatted near 20°C, thermal expansion corrections were negligible. McGlashan<sup>26</sup> has discussed a correction arising from the fact that the thermostat window may not be vertical. For the apparatus used, this correction (found by measuring difference in height between the two menisci with both sides of the manometer evacuated) was less than 0.01 mm Hg for all temperatures and was independent of the mercury height.

Fig. 2.7.4

Apparatus for Observing Meniscus



Corrections to the observed pressure

The measured height difference between two mercury levels depends upon the local value of the acceleration due to gravity and mercury density. This height difference has to be corrected since pressure is defined in terms of the height difference when mercury is at 0°C and acceleration due to gravity equals  $980.665 \text{ cm sec}^{-2}$ <sup>84,83</sup>. Mercury density data at different temperatures were taken from the Handbook of Chemistry and Physics,<sup>39</sup> while the local acceleration due to gravity was calculated from

$$g = 978.039(1 + 0.005294 \sin^2 \phi - 0.000007 \sin^2 2\phi) - 0.00009406 H \quad \dots \quad (2.7.4)$$

where  $\phi$  is the latitude and H is the height in feet above sea level<sup>83</sup>. The calculated value has been shown to differ by as much as  $0.2 \text{ cm sec}^{-2}$  from the experimental value - this difference could produce an error of 0.16 mm Hg in a measured pressure of 760 mm Hg. The g-value has not been measured in Armidale. Values used are summarised in Table 2.7.1.

TABLE 2.7.1

$g = 979.308 \text{ cm sec}^{-2}$			
<u>Density of mercury</u>			
Temp (°C)	Density (g/ml)	Temp (°C)	Density (g/ml)
0	13.5955	45	13.4851
25	13.5340	50	13.4729
30	13.5217	55	13.4608
35	13.5095	60	13.4486
40	13.4973	65	13.4365

The vapour pressure at the surface of the liquid in the cell

differs from the measured vapour pressure. The correction equals  $+ h\rho$  where  $h$  is the height of the liquid below the mercury meniscus and  $\rho$  is the vapour density. This correction was calculated to be less than 0.005 mm Hg. for all the situations encountered. All measurements were made with one side of the manometer continually evacuated.

#### Pure materials - vapour pressure

Vapour pressures of pure components were measured at 25°, 30°, 35°, 40°, 45°, 50°, 55°, and 60°C. The ampoules, prepared as described previously in Chapter 2.2, were sealed into ampoule holders shown in Fig. 2.7.1. After evacuation, this section of the vacuum line was checked for leaks and the ampoule holder area, manometer and vapour pressure bulb were thoroughly degassed by flaming and pumping. To prevent overheating, the sample was frozen prior to flaming. The degassing process was continued for at least 24 hours, gassing being then checked by the sensitive Pirani gauge. This outgassing was especially important as any further degassing after the introduction of the sample could cause erroneous results. After closing teflon taps T1 and T2 and adjusting the mercury to a level just below the U-bend of the manometer, the breakseal of the ampoule was broken.

The liquid was distilled into the vapour pressure bulb by immersing the bulb in liquid air. On completing distillation, mercury was forced into the manometer and the apparatus lowered into the 25°C bath. Measurements were usually made at three temperatures within

0.05°C of the desired temperature. The pressure at a rounded temperature was interpolated from a large scale graph.

To check that equilibrium had been reached, measurements were made after increasing and after decreasing the temperature. Constancy in measurements showed that equilibrium had been attained in less than a half hour after a small temperature adjustment, and in less than two hours after a large (5° or 10°C) temperature change. To assist attainment of equilibrium the liquid in the vapour pressure cell was stirred, using a glass-enclosed steel plunger which was moved up and down by the switching of a solenoid - insert Fig. 2.7.1. The solenoid was switched by contacts moving over a number of metal plates connected to the face of a wooden pulley mounted on a motor. The frequency of switching was altered by varying the speed of the motor with a Variac. The plunger's lower end was shaped to act as a pump during its upward travel. The liquid surface was thus continually broken and liquid was sprayed over the walls of the cell. This stirring process was found much more effective than the normal type of magnetic stirrer floating on the surface, since the floating type inevitably broke on freezing the liquid.

After the completion of measurements over the temperature range to 60°C, a check measurement was made at 25°C. Agreement within 0.02 mm Hg of the initial value in all cases indicated that the outgassing process was complete. Purity was checked by pumping off half the sample and remeasuring the vapour pressure at 25°C and 60°C. It was further checked by measuring vapour pressures of the first and last ampoules

prepared.

Initial design of the manometer and vapour pressure cell proved unsatisfactory because of distillation of liquid onto the mercury surface - this phenomenon can only occur with pure components and not with mixtures. By placing all parts of the vapour pressure side of the manometer at least eight inches below the water surface, the effect was considerably reduced. It was suspected that slight temperature fluctuations near the water surface gave rise to the distillation.

#### Mixtures - vapour pressure

##### Determination of total composition

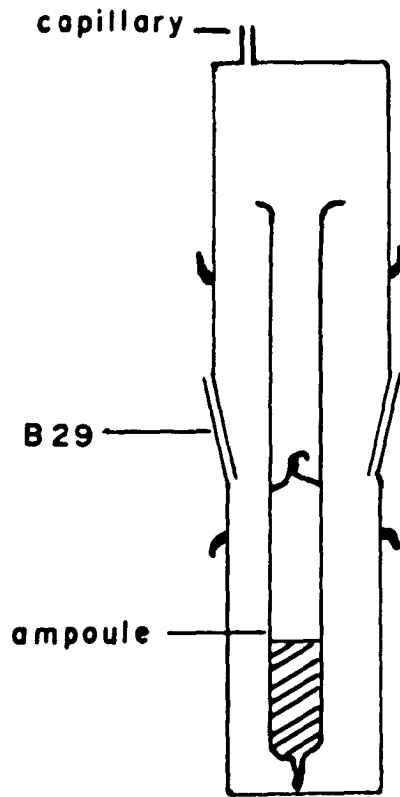
It was necessary to distil into the vapour pressure cell known masses of each component. The following technique was used: ampoules were thoroughly cleaned and equilibrated in a thermostatted balance room for an half hour before weighing on a Mettler semi-micro balance (B6H26 - accuracy  $\pm 0.02$  mg ). Great care was taken to develop reproducible weighing conditions. External volumes of the ampoules, needed for buoyancy correction to weighings, were determined using the density bottle shown in Fig. 2.7.5. The volume of the ampoule could be determined to within 0.005 ml.

After the weighing and volume determination, the ampoule was inserted into its holder, the latter being then sealed into the vacuum line. The whole ampoule area was then outgassed.

To prevent excessive scattering of broken glass when opening the

Fig. 2.7.5

Density Bottle



ampoule, the ampoule was frozen prior to breaking. The shape was such that any broken glass fell back into the ampoule and not into the holder. Distillation of the volatile substances into the vapour pressure bulb required special care since sufficiently high pressures could cause a vapour loss if the mercury was forced low enough to allow vapour to escape into the lower mercury bulb. The pressure above the mercury could be controlled with tap T2. The Pirani gauge was used to check that distillation was complete.

After introducing two components in this manner, the mercury level was raised into the mercury cut-off manometer, T2 was closed and the apparatus lowered into the bath, to reach equilibrium prior to a 25°C measurement. During equilibration, ampoule holders were broken open, and the ampoule (with the broken glass) were removed and weighed. On rare occasions, breakage of the holder introduced small pieces of broken glass but these were distinguishable from breakseal glass owing to their shape. Glass pieces were observed under a magnifying glass before and after breakage.

The weight in vacuum was calculated from

$$W_v = W' - W'' + V_t \rho'_a - V_g \rho''_a - \frac{W' \rho'_a}{\rho_w} + \frac{W'' \rho''_a}{\rho_w} \quad \dots \quad (2.7.5)$$

$W_v$  = weight of sample in vacuum

$W'$  = weight of ampoule with liquid

$W''$  = weight of ampoule when empty

$\rho'_a$  = density of air when weighing ampoule with liquid

$\rho''_a$  = density of air when weighing empty ampoule

$V_t$  = total volume of ampoule

$V_g$  = volume of the glass comprising the ampoule  
 =  $W''/\rho_g$

$\rho_g$  = density of glass (2.23g/ml )

$\rho_w$  = density of the stainless steel weights (7.8g/ml )

Weighings were considered accurate to 0.1 mg.

After weighing an empty ampoule, another weighed ampoule was immediately sealed into a holder and degassing was continued while the vapour pressure of the first mixture was measured at 25°, 35°, 45°, 55° and 60°C. A check measurement at 25°C was always done before introducing the next sample. This process was continued until the desired concentration range was covered.

To calculate solution composition it was essential to know the volume available to the vapour. The total vapour space of the vapour pressure bulb, up to the mercury surface, was determined in two ways. Firstly, an amount of nitrogen was introduced into the cell, its pressure being determined with the mercury level at a known distance from a reference mark (taken as the lower edge of a square clamp holding the manometer in position). Nitrogen was then compressed by moving mercury up the manometer. From the measured change in volume (calculated from mercury height changes and precision bore diameter) and the measured

pressure change, the volume to the reference mark could be calculated.

Secondly, the volume was determined by blowing small holes in the glass and filling the manometer with water from a weightburet. From the mercury height relative to the reference mark and mass of water added, the volume of the vapour pressure cell to the reference mark was again determined. Results appear in Table 2.7.2, showing agreement of the two methods within  $\pm 0.4$  ml.

TABLE 2.7.2

<u>Volume of vapour pressure cell to reference mark</u>	
A By compression	118.3 ml
	119.0
	118.8
	117.6
B By weighing in water	<u>118.34</u>
Av. volume	<u>118.4 ml</u>

Difficulties with carbon tetrachloride

Carbon tetrachloride vapour reacts with mercury to form tide marks on the glass surface of a manometer<sup>85</sup>. It has been suggested that the reaction is due to the production of static electricity as mercury moves over the dry glass surface. The above phenomenon obviously made accurate pressure measurements difficult. The effect was minimised as follows: measurements were made from 25° through to 60°C, and

repeated at 25°, with the mercury meniscus always rising. Initial measurements were made with the mercury at the lowest possible level. It was found that the scum was left on the walls and a reasonably clean surface resulted.

After completion of a series of measurements the manometer was raised from the bath, the sample frozen in liquid air and the mercury level lowered below the U bend. Gentle flaming of the whole manometer area caused the scum to sublime down to the bottom of the manometer, leaving the glass surface clean. By rapidly raising the mercury, a clean mercury surface was obtained.

The sample freezing and flaming procedure was repeated three times with pure carbon tetrachloride. Agreement of the vapour pressures at 25°C and 60°C indicated that the process had no detrimental effects. With one of the mixtures the above process was repeated and constancy in the vapour pressure was observed. Hence, it was concluded that the amount of decomposition, although noticeable by the scum, was very small indeed.

Reliability of vapour pressure measurements on the carbon tetrachloride-OMCTS system was considered lower than that on the benzene-OMCTS system. The above difficulty with carbon tetrachloride could easily be overcome by using a nulling manometer to separate the mixture from the mercury manometer.

CHAPTER 3RESULTS3.1 INTRODUCTION

In this chapter the experimental results are listed for the following properties; density, viscosity, diffusion coefficients and activity coefficients for the systems OMCTS - benzene and OMCTS - carbon tetrachloride.

In some cases the full experimental results have not been included for the sake of brevity (e.g. refractive index gradients from the Gouy diffusimeter measurements).

3.2 PURIFICATION OF MATERIALSBenzene

The purity of benzene used for vapour pressure measurements was determined by its freezing point, refractive index and vapour pressure. Table 3.2.1 compares the freezing point of the final benzene sample with literature values.

Equipment available precluded accurate refractive index measurements. The refractive index of the final sample agreed with literature results. Measurements were made at 25°C using the sodium D line with a Bellingham and Stanley Abbe refractometer. Results are given in Table 3.2.2.

TABLE 3.2.1

<u>Freezing Point of Benzene</u>	<u>Temp. (°C)</u>
This work - final sample	5.518
This work - mother liquors	5.515
Davison <sup>86</sup> (1945)	5.496
Streiff and Rossini <sup>87</sup> (1944)	5.530
Forziati et al. <sup>88</sup> (1946)	5.533
Rybicka and Wynne-Jones <sup>33</sup> (1950)	5.525

TABLE 3.2.2

<u>Refractive Index of Benzene at 25°C</u>	<u><math>n_D^{25}</math></u>
This work	1.4979
Forziati et al. <sup>89</sup>	1.49792
Campbell and Miller <sup>90</sup>	1.4979

Vapour pressure results are recorded in Appendix II. As the pressure measurements were not made at rounded temperatures, consistency was checked by comparing deviations from the National Bureau of Standards Antoine equation<sup>91</sup>. Table 3.2.3 summarises the experimental

and literature values at the rounded temperatures,<sup>91,35,92,28,27</sup> while Fig. 3.2.1 illustrates the deviation of experimental measurements from the above equation. Careful examination of the available data for benzene suggests that the Antoine equation quoted in the Bureau of Standards tables gives values which are of the order of 0.10 to 0.20mm Hg low in the intermediate temperature range 35° to 60°C. Everett et al.<sup>27</sup> reached a similar conclusion. Experimental results were fitted to a new Antoine equation with the aid of a computer programme (Appendix II). The following equation gave the best fit,

$$\log_{10} p = 6.905874 - 1210.719/(220.721 + t) \quad \dots (3.2.4)$$

Further examination of Fig. 3.2.1 reveals that the results presented in this thesis may be slightly high at 55°C. It should be noted that the results of Scatchard, Smith and Rossini were obtained with a recirculating still. Scatchard has attributed the discrepancies at low temperatures to deficiencies in the design of the recirculating still<sup>35</sup>.

### Carbon tetrachloride

The refractive index of the sample ( $n_D^{25} = 1.4603$ ) agreed with the most precise results quoted in Timmermans<sup>93</sup>. Experimental results for the vapour pressure of carbon tetrachloride are tabulated in Appendix II. In Table 3.2.4 the vapour pressure results at rounded temperatures are compared with literature data<sup>34,35</sup>. Deviations from Scatchard's equation,

TABLE 3.2.3

Vapour Pressure of Benzene at Rounded Temperatures (in mm Hg)

Temp (°C)	This work	Scatchard (a)	Smith (b)	Rossini (c)	Baxendale	Everett
25	95.20	94.98	95.27	95.18	95.27	95.31
30	119.38	119.17	119.44	119.34	119.40	-
35	148.37	148.18	148.42	148.31	-	148.51
40	182.87	182.72	182.91	182.79	182.69	-
45	223.64	223.49	223.64	223.51	-	223.54
50	271.44	271.34	271.42	271.29	271.40	-
55	327.22	327.10	327.11	326.97	-	327.39
60	391.70	391.66	391.60	391.48	391.62	-
(a)	$\log_{10}P = 6.66457 - 1007.742/T - 116197/T^2$				... (3.2.1)	
(b)	$\log_{10}P = 6.905216 - 1211.215/(220.870 + t)$				... (3.2.2)	
(c)	$\log_{10}P = 6.905650 - 1211.033/(220.790 + t)$				... (3.2.3)	

TABLE 3.2.4

Vapour Pressure of Carbon tetrachloride at Rounded Temperatures (in mm Hg)

Temp (°C)	This work	Brown	Scatchard
25	114.23	-	113.89
30	141.93	141.55	141.55
35	174.80	-	174.47
40	213.64	213.42	213.35
45	259.17	-	258.93
50	312.20	321.23	312.04
55	373.58	-	373.52
60	444.21	444.44	444.28

Fig. 3.2.1

Vapour Pressure of Benzene

Deviation from N.B.S. Antoine Equation

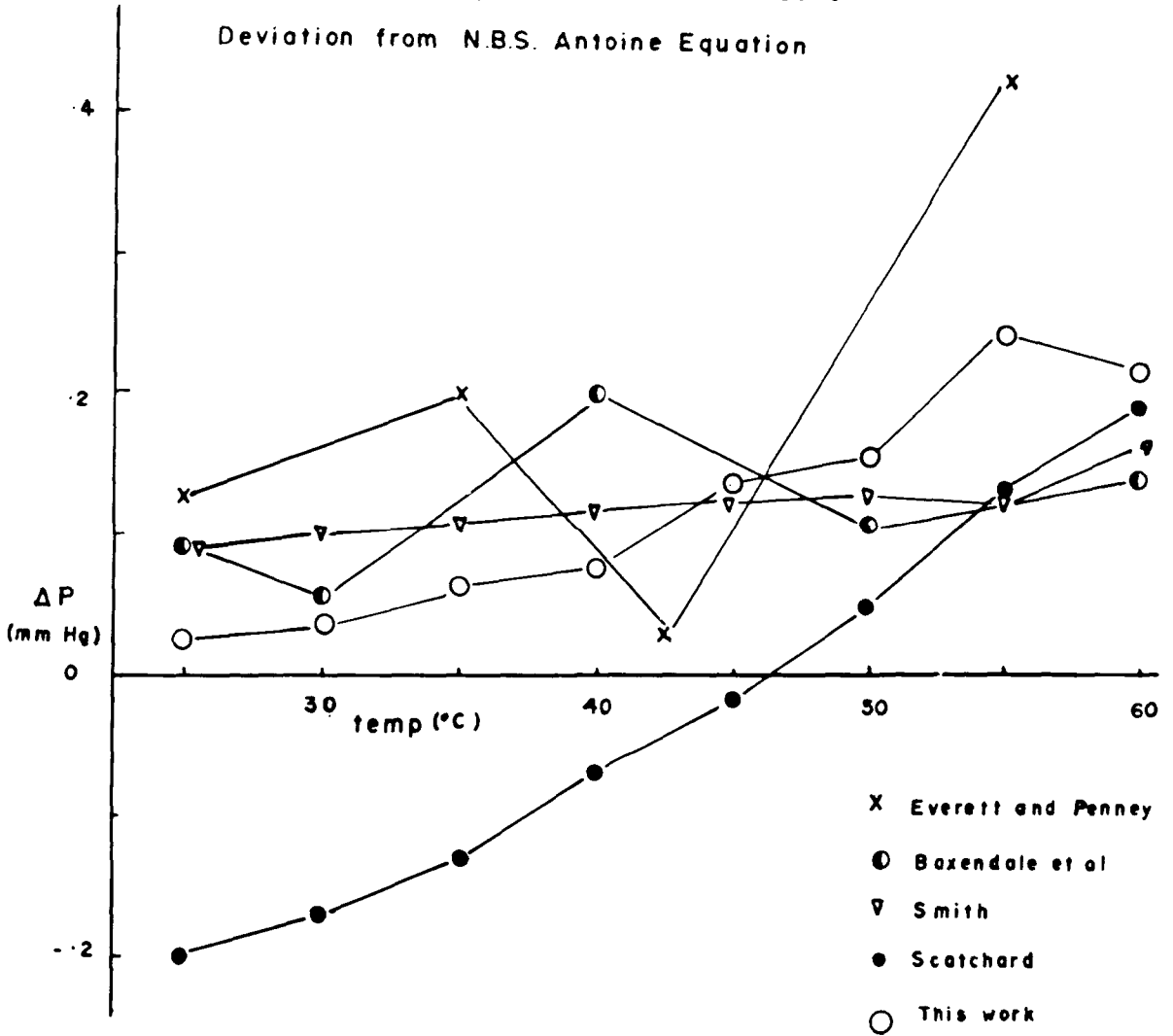
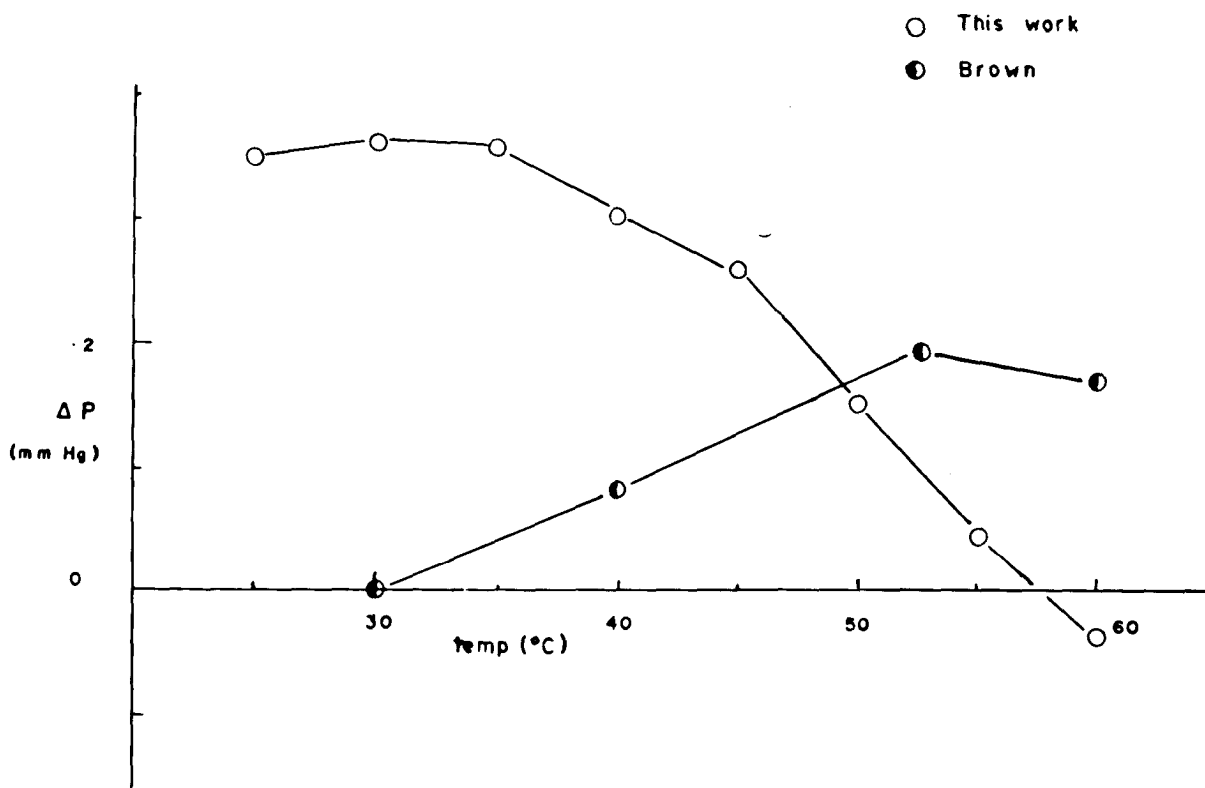


Fig. 3.2.2.  
Vapour Pressure of  $\text{CCl}_4$   
Deviation from Scatchard Equation



$$\log_{10}P = 6.68148 - 1045.022/T - 99577/T^2 \quad \dots \quad (3.2.5)$$

are shown in Fig. 3.2.2. Deviations are significant at low temperatures, but it should be noted that both Scatchard and Brown used a recirculating still.

Equation 3.2.6 fitted all the experimental data from 25° to 60°C to within  $\pm 0.02$  mm Hg,

$$\log_{10}P = 6.84893 - 1194.501/(224.315 + t) \quad \dots \quad (3.2.6)$$

#### Octamethylcyclotetrasiloxane

The measured refractive index ( $n_D^{25} = 1.3968$ ) agreed with the result of Patnode and Wilcock<sup>29</sup>. In Appendix II the vapour pressure results are given, and values interpolated at rounded temperatures are compared with literature data<sup>31,94</sup> in Table 3.2.5. Vapour pressures over the range 25° to 60°C were fitted by the equation,

$$\log_{10}P = 7.61674 - 1804.28/(211.81 + t) \quad \dots \quad (3.2.9)$$

to within  $\pm 0.01$  mm Hg.

It should be noted that vapour pressure results for all aforementioned substances may be in error slightly because of an uncertainty of the value of acceleration due to gravity,  $g$ , at Armidale.

TABLE 3.2.5

Vapour Pressure of OMCTS at Rounded Temperatures (in mm Hg)

Temp (°C)	This work	Ostoff and Grubb (a)	Jordan (b)
25	1.00	0.93	1.26
35	2.02	1.92	2.45
45	3.89	3.74	4.54
55	7.14	7.14	8.06
60	9.52	9.27	10.57
	(a) $\log_{10}P = 45.7216 - 4530.2/T - 12.3508 \log_{10}T \quad \dots \quad (3.2.7)$		
	(b) $\log_{10}P = 7.6010 - 1868.9/(224.17 + t) \quad \dots \quad (3.2.8)$		

### 3.3 DENSITY RESULTS

Densities, excess densities and excess volumes for the systems studied are tabulated in Tables 3.3.1, 3.3.2 and 3.3.3. Included are the values calculated with and without the pycnometer vapour space correction. This correction was found to be small for the OMCTS - benzene system but significant in the OMCTS - carbon tetrachloride system. That the above correction needs to be considered is indicated by the agreement of corrected results with those obtained by the flask pycnometer for the latter system. Disagreement between OMCTS - benzene results by the two methods is disturbing. It appears however, that some of the experimental results may be in error, particularly at the high silicone concentration. In giving the system more detailed attention, the use of a dilatometer would be preferred over the density technique used in this work.

Excess volumes for the OMCTS - benzene system were found to be small and almost independent of temperature; viz,  $V^E = -0.029 \text{ ml mole}^{-1}$  at  $x_1 = 0.23$  at  $25^\circ\text{C}$ ,  $V^E = -0.04 \text{ ml mole}^{-1}$  at  $x_1 = 0.25$  at  $60^\circ\text{C}$ . Results at  $25^\circ\text{C}$  were fitted to an equation suggested by Scott,<sup>104</sup>

$$V^E = \frac{x_1 x_2}{1 - D(1 - 2x_2)} [A + B(1 - 2x_2) + C(1 - 2x_2)^2 + \dots] \dots (3.3.1)$$

The coefficients which gave the best fit to  $\pm 0.002 \text{ ml mole}^{-1}$  were;

$$A = - 0.03194$$

$$B = 0.1710$$

$$C = - 0.0674$$

$$D = - 0.100$$

In the system OMCTS - carbon tetrachloride, excess volumes were large and negative but again varied only slightly with temperature, ( $V^E = - 0.217 \text{ ml mole}^{-1}$  at  $25^\circ\text{C}$  and  $V^E = - 0.235 \text{ ml mole}^{-1}$  at  $60^\circ\text{C}$  at  $x_1 = 0.179$ ). Coefficients of equation 3.3.1 giving a fit to  $\pm 0.003 \text{ ml mole}^{-1}$  were:

$$A = - 1.005$$

$$B = 0.8459$$

$$C = - 0.2298$$

$$D = 0.250$$

The densities of OMCTS at  $25^\circ$ ,  $35^\circ$ ,  $45^\circ$ ,  $55^\circ$  and  $60^\circ\text{C}$  are given in Table 3.3.4. The data fitted equation 3.3.2 with an average deviation of  $0.000003 \text{ g ml.}^{-1}$

$$\rho_1^t = \rho_1^{25} - 1.1423 \times 10^{-3}(t - 25) - 2.3735 \times 10^{-7}(t - 25)^2 \dots (3.3.2).$$

TABLE 3.3.1

Densities of Mixtures OMCTS(1) - Benzene(2)

$\phi_1$	$x_1$	$\rho_{\text{meas}}$	$\Delta \times 10^5$ (no vapour corr.)	$V^E$	$\Delta \times 10^5$ (vapour corr. included)	$V^E$
<u>Ostwald-Sprengel pyknometer</u>						
.11834	.03705	.88257	8	-.009	7	-.008
.21495	.07276	.89006	12	-.014	11	-.013
.32097	.11931	.89830	18	-.023	17	-.022
.46634	.20029	.90953	19	-.028	18	-.027
.56948	.27489	.91746	16	-.027	15	-.025
.65412	.35149	.92396	13	-.024	12	-.022
.78745	.51498	.93415	4	-.008	3	-.006
.87299	.66329	.94070	-1	.003	-2	.005
		$\rho_1^{\circ} = .95051$	$\rho_2^{\circ} = .87336$			
<u>Flask pyknometer</u>			(no vapour corr. necessary)			
.48566	.21291	.911087	15	-.023		
.54474	.25527	.915619	14	-.024		
		$\rho_1^{\circ} = .950429$	$\rho_2^{\circ} = .873641$			
Density units-g/ml						
Excess volume units - ml mole <sup>-1</sup>						

TABLE 3.3.2

Densities of Mixtures OMCTS(1) - Carbon tetrachloride(2)

$\phi_1$	$x_1$	$\rho_{\text{meas}}$	$\Delta \times 10^5$ (no vapour corr.)	$V^E$	$\Delta \times 10^5$ (vapour corr. included)	$V^E$
<u>Ostwald - Sprengel pycnometer</u>						
.04194	.01343	1.55834	38	-.024	39	-.025
.07252	.02374	1.53922	65	-.043	67	-.044
.14488	.05006	1.49372	103	-.075	107	-.078
.23419	.08686	1.43749	144	-.116	150	-.121
.32417	.12983	1.38087	188	-.170	197	-.178
.41278	.17943	1.32481	201	-.206	211	-.217
.42077	.18431	1.31973	200	-.207	210	-.217
.48787	.22859	1.27712	194	-.222	206	-.235
.51999	.25204	1.25672	191	-.230	203	-.244
.54269	.26962	1.24238	197	-.245	208	-.260
.61462	.33159	1.19656	175	-.247	188	-.264
.74652	.47811	1.11251	135	-.243	147	-.264
.79790	.55119	1.07962	104	-.208	115	-.230
.81059	.57104	1.07151	98	-.201	108	-.222
.86711	.66994	1.03538	69	-.161	78	-.181
		$\rho_1^{\circ} = .95042$	$\rho_2^{\circ} = 1.58456$			
<u>Flask pycnometer</u>						
			(no vapour corr. required)			
.41227	.17912	1.325202	212	-.217		
		$\rho_1^{\circ} = .950429$	$\rho_2^{\circ} = 1.584485$			
Density units-g/ml						
Excess volume units - mlmole <sup>-1</sup>						

TABLE 3.3.3Excess Volumes at 60°C - Flask Pyknometer

$\phi_1$	$x_1$	$\rho_1^o$	$\rho_2^o$	$\rho$	$\Delta \times 10^5$	$V^E$
<u>OMCTS(1) - benzene(2)</u>						
.48540	.21291	.91016	.835761	.872109	23.3	-.038 <sub>3</sub>
.54448	.25527	.910162	.835761	.876504	23.3	-.040 <sub>6</sub>
<u>OMCTS(1) - carbon tetrachloride(2)</u>						
.41194	.17912	.910162	1.515303	1.26812	210.2	-.234 <sub>9</sub>
density units - g/ml excess volume units - ml mole <sup>-1</sup>						

TABLE 3.3.4OMCTS - Variation of Density with Temperature

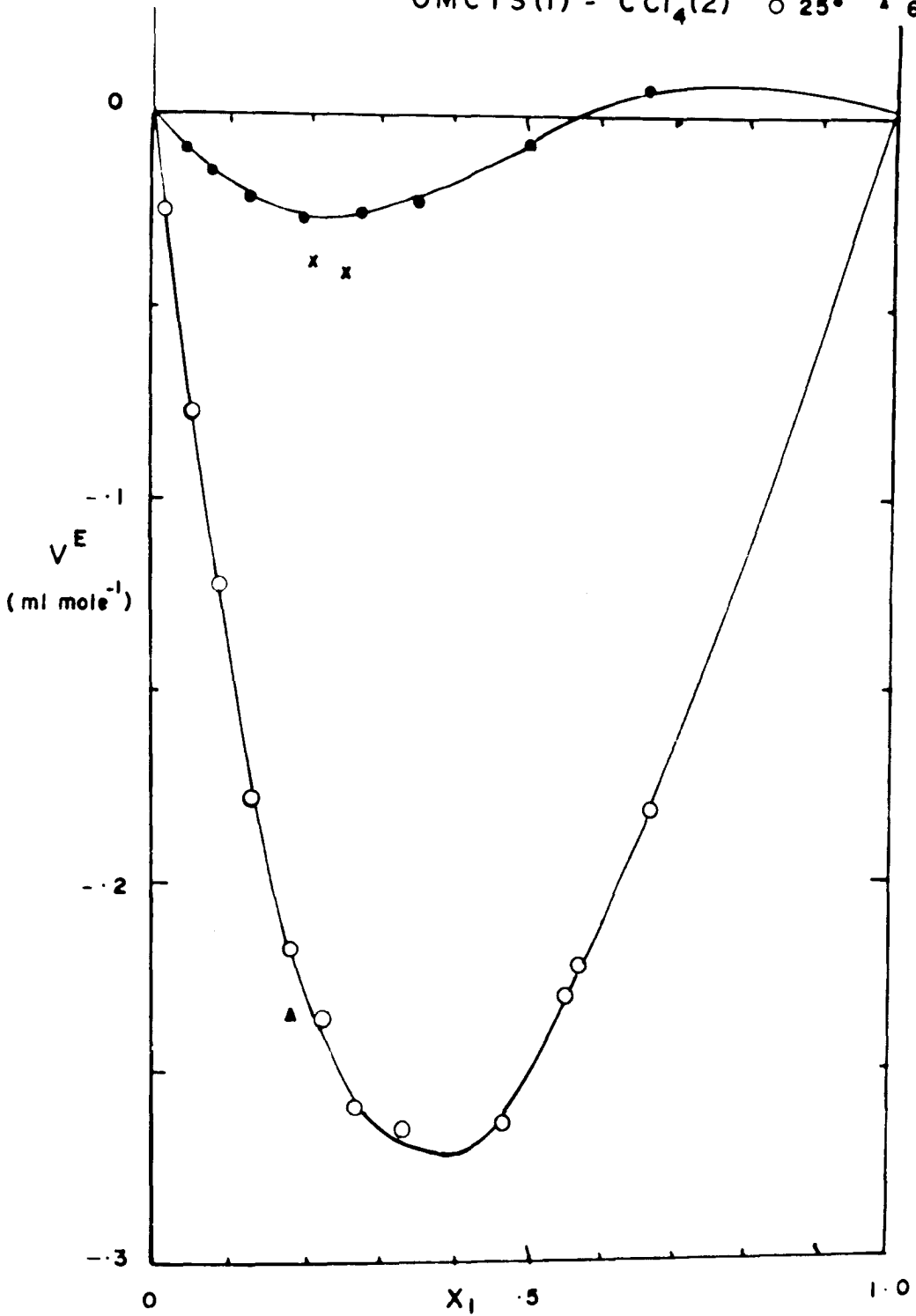
Temp (°C)	Density (g/ml)
25	.950429
35	.938984
45	.927491
55	.915940
60	.910162

Fig. 3.3.1

Excess Volumes

OMCTS(1) - C<sub>6</sub>H<sub>6</sub>(2) • 25° x 60°C

OMCTS(1) - CCl<sub>4</sub>(2) ○ 25° ▲ 60°C



### 3.4 VISCOSITY RESULTS

Viscosity results at 18°, 25°, 35° and 45°C for the two mixtures studied are given in Tables 3.4.1 and 3.4.2. The deviation  $\Delta\eta$  given by,

$$\Delta\eta = \eta_{\text{calc}} - \eta_{\text{exp}}$$

where

$$\eta_{\text{calc}} = x_1 (\eta_1 - \eta_2) + \eta_2 \quad \dots (3.4.1)$$

are included in the tables. The variation of  $\Delta\eta$  with concentration for the two systems are shown in Fig. 3.4.1 and 3.4.2. Viscosities at specific mole fractions were calculated from equation 3.4.1 and the interpolated values of  $\Delta\eta$ . The viscosity of OMCTS at 25°C (2.191 cp) agreed with the value quoted by Hurd<sup>95</sup> (2.192 cp). This latter value has been corrected for the more recent viscosity value for water at 25°C. In Table 3.4.3 viscosities of benzene at 18°, 25°, 35° and 45°C are compared with the values quoted in Table 5C of Selected Values of Properties of Hydrocarbons and Related Compounds<sup>96</sup>. Except at 18°C, the two sets of data agree to better than 0.25%. In the following tables viscosities and viscosity deviations are recorded in centipoise.

TABLE 3.4.1Viscosities OMCTS (1) - Benzene (2)

Temp	$x_1$	$\eta$	$\Delta\eta$	Temp	$x_1$	$\eta$	$\Delta\eta$
18°C	.0881	.7346	.098 <sub>6</sub>	35°C	.0886	.5768	.060 <sub>3</sub>
	.3511	1.0591	.261		.3517	.818	.156
	.5997	1.493	.287		.6020	1.127	.168
	.7738	1.885	.217		.7741	1.390	.126
	.8529	2.091	.157		.8544	1.527	.092
	.9369	2.328	.075		.9373	1.682	.043
25°C	.0341	.6224	.0541	45°C	.0888	.5068	.046 <sub>9</sub>
	.0699	.6486	.0648		.3526	.7140	.117 <sub>6</sub>
	.1407	.7099	.116		.6036	.9714	.124 <sub>8</sub>
	.2235	.7944	.163		.7763	1.186	.092
	.2938	.8750	.195		.8562	1.298	.065
	.3751	.9814	.217		.9134	1.393	.030
	.4689	1.1128	.234				
	.6211	1.3629	.227				
	.6777	1.4664	.213				
	.7510	1.608	.187				
	.8434	1.804	.138				
	.8753	1.880	.113				
	.9028	1.939	.097				
	.9291	2.010	.068				

Viscosity units - centipoise

TABLE 3.4.2Viscosities OMCTS (1) - Carbon tetrachloride (2)

Temp	$x_1$	$\eta$	$\Delta\eta$	Temp	$x_1$	$\eta$	$\Delta\eta$
18°C	.1780	1.256	.016	35°C	.1756	.964	-.002
	.3227	1.448	.044		.3239	1.101	.012
	.5718	1.798	.071		.5732	1.339	.030
	.7258	2.036	.068		.7290	1.493	.035
	.8618	2.268	.042		.8636	1.646	.020
	.9815	2.488	.004		.9817	1.786	.001
25°C	.1089	1.0437	-.003	45°C	.1779	.844	-.002
	.1965	1.1404	.012		.3249	.956	-.001
	.2890	1.245	.026		.5816	1.148	.020
	.4288	1.407	.042		.7307	1.270	.021
	.5841	1.595	.053		.8652	1.388	.015
	.6590	1.694	.050		.9821	1.498	.001
	.8443	1.950	.031				
	.9264	2.073	.013				
	.9773	2.147	.004				

Viscosity units -  
centipoise

Fig. 3.4.1  
Viscosity Deviation  
OMCTS (1) - C<sub>6</sub>H<sub>6</sub> (2)

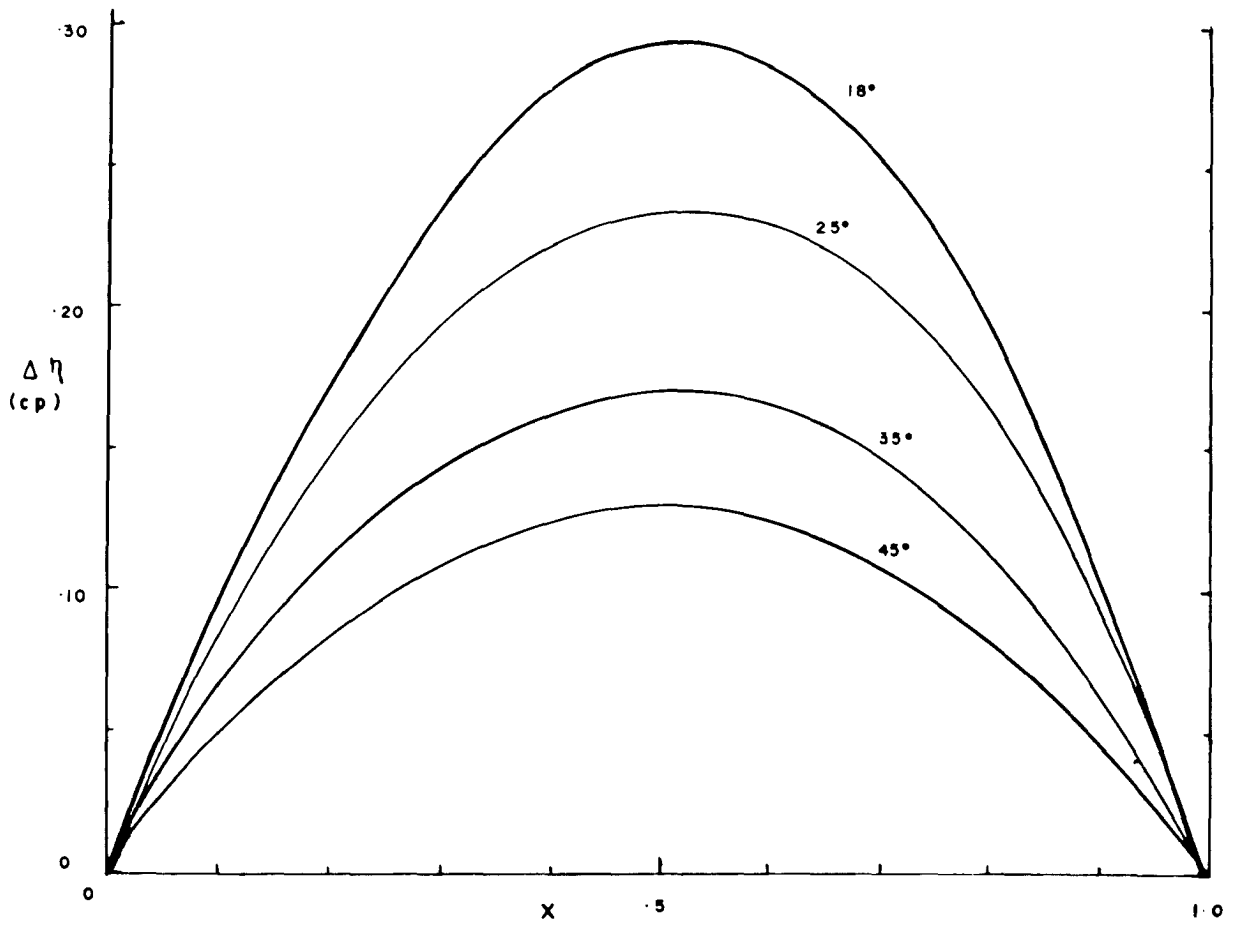


Fig. 3.4.2

Viscosity Deviation

OMCTS (1) -  $\text{CCl}_4$  (2)

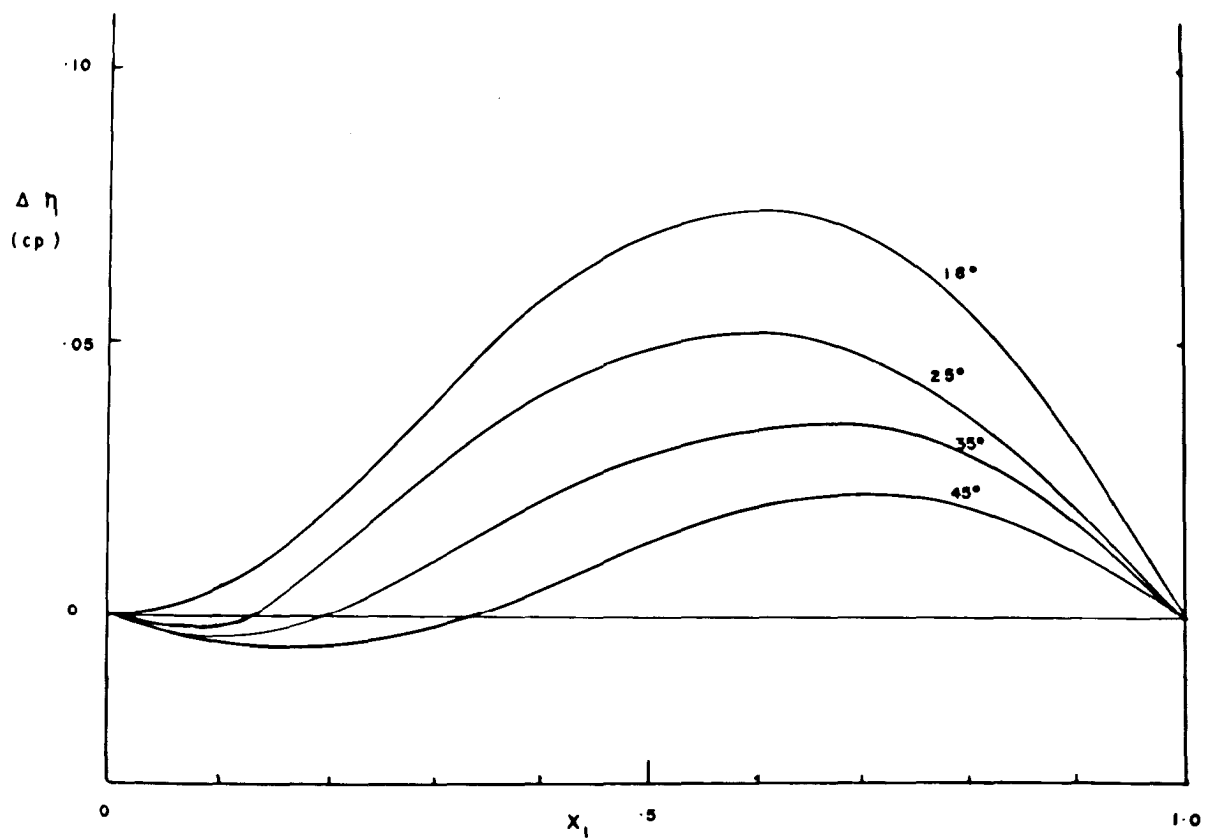


TABLE 3.4.3Viscosity of Benzene

Temp (°C)	$\eta_2$ (exp.)	$\eta_2$ (A.P.I.)
18	.6703	.6674
25	.6024	.6010
35	.5235	.5236
45	.4603	.4615

Viscosity of OMCTS and Carbon tetrachloride

Temp (°C)	$\eta$ OMCTS	$\eta$ CCl <sub>4</sub>
18	2.520	1.001
25	2.190	.901 <sub>1</sub>
35	1.806	.781 <sub>7</sub>
45	1.514	.686 <sub>6</sub>

Viscosity units - centipoise

### 3.5 DIFFUSION RESULTS

Mutual diffusion coefficients obtained with the Gouy diffusimeter are given in Tables 3.5.1 and 3.5.2. Results are shown graphically in Figs. 3.5.1 and 3.5.2. Diaphragm cell results are given in Table 3.5.3 while diffusion coefficients extrapolated to  $x_1 = 0$  and  $x_1 = 1$  at the various temperatures for the two systems studied are tabulated in Table 3.5.4. The mutual diffusion coefficients determined with the diaphragm cell are, on the average, 1.5% higher than the Gouy results. Discrepancies between optical and diaphragm cell results have been noted in the literature<sup>97</sup>. Diffusion coefficients determined by the Gouy method are considered accurate to 0.2%. The units of the diffusion coefficients listed in the following tables are ( $\text{cm}^2 \text{sec}^{-1} \times 10^{-5}$ ).

TABLE 3.5.1

Mutual Diffusion Coefficients OMCTS (1) - Benzene (2)

Temp	$x_1$	$D_{12}$	Temp	$x_1$	$D_{12}$	Temp	$x_1$	$D_{12}$
18°C	.0031	1.005	25°C	.4767	1.176	45°C	.0031	1.576
	.0237	.967		.5494	1.177		.0237	1.538
	.0795	.908		.6006	1.181		.0795	1.483
	.1388	.905		.6578	1.182		.1388	1.484
	.2304	.931		.7814	1.169		.2304	1.537
	.3227	.968		.8672	1.146		.3227	1.601
	.5029	1.022		.9098	1.129		.5029	1.693
	.6432	1.030		.9630	1.111		.6432	1.715
	.7539	1.015		.9714	1.104		.7539	1.711
.9571	.959			.9571	1.645			
25°C	.0031	1.145	35°C	.0031	1.350	$D_{12}$ units - $\text{cm}^2 \text{sec}^{-1} \times 10^{-5}$		
	.0033	1.147		.0237	1.308			
	.0237	1.101		.0795	1.249			
	.0460	1.080		.1388	1.248			
	.0795	1.042		.2304	1.288			
	.1085	1.033		.3227	1.343			
	.1388	1.036		.5029	1.419			
	.1706	1.046		.6432	1.439			
	.2304	1.066		.7539	1.429			
	.2617	1.087		.9571	1.358			
	.3227	1.126						
.3489	1.134							

TABLE 3.572

Mutual Diffusion Coefficients OMCTS (1) - Carbon tetrachloride (2)

Temp	$x_1$	$D_{12}$	Temp	$x_1$	$D_{12}$	Temp	$x_1$	$D_{12}$
18°C	.0048	.6420	25°C	.4627	.8578	45°C	.0048	1.017
	.1211	.6715		.4733	.8591		.1211	1.085
	.2349	.7084		.5407	.8603		.2349	1.151
	.3617	.7394		.5882	.8627		.3617	1.210
	.4882	.7491		.6703	.8565		.4882	1.245
	.7000	.7456		.7375	.8495		.7000	1.259
	.8159	.7310		.7939	.8435		.8159	1.259
	.9536	.7068		.8763	.8348		.9536	1.231
				.9487	.8204			
25°C	.0038	.7228	35°C	.0048	.867	$D_{12}$ units - $\text{cm}^2 \text{sec}^{-1} \times 10^{-5}$		
	.0208	.7288		.1211	.920			
	.0375	.7333		.2349	.974			
	.0493	.7366		.3617	1.019			
	.0667	.7430		.4882	1.044			
	.1188	.7604		.7000	1.049			
	.1338	.7695		.8159	1.038			
	.1627	.7795		.9536	1.012			
	.1952	.7915						
	.2244	.8070						
	.2592	.8170						
	.2987	.8298						
	.3455	.8380						
	.3866	.8502						

TABLE 3.5.3Diffusion Coefficients Diaphragm Cell - 25°C

Cell	$\bar{c}_1$	$\bar{x}_1$	D (diaph.)	D (Gouy)
<u>Diphenyl (1) - Benzene (2)</u>				
[D <sub>12</sub> units - cm <sup>2</sup> sec <sup>-1</sup> x 10 <sup>-5</sup> ]				
GB1	.612		1.437	1.425
UB1	.346		1.469	1.482
				(from ref. 23)
<u>OMCTS (1) - Carbon tetrachloride (2)</u>				
G01	.170	.0155	.739	.728
A01	.175	.0150	.741	.729
X010	.271	.0250	.747	.731
U010	.524	.0530	.748	.740
U011	.684	.0718	.757	.746
$\bar{c}$ - average concentration in mole l <sup>-1</sup>				

TABLE 3.5.4Extrapolated Diffusion Coefficients

Temp (°C)	D (x <sub>1</sub> = 0)	D (x <sub>2</sub> = 1)
<u>OMCTS (1) - Benzene (2)</u>		
[D <sub>12</sub> units - cm <sup>2</sup> sec <sup>-1</sup> x 10 <sup>-5</sup> ]		
18	1.011	.942
25	1.152	1.085
35	1.352	1.341
45	1.579	1.632
<u>OMCTS (1) - Carbon tetrachloride (2)</u>		
18	.641	.693
25	.722	.810
35	.865	1.003
45	1.015	1.230

Fig. 3.5.1

Mutual Diffusion Coefficients

OMCTS(1) -  $C_6H_6$ (2)

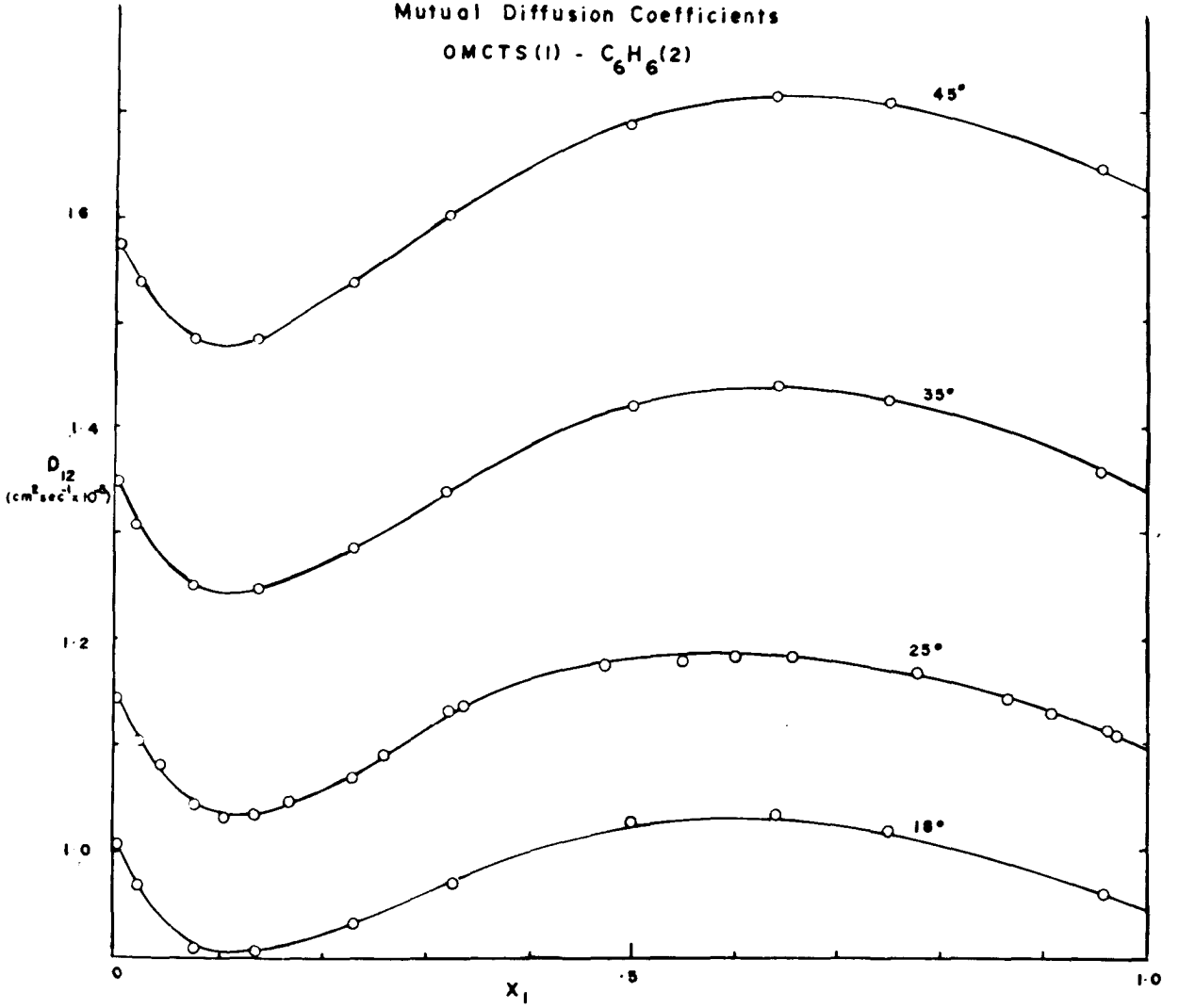
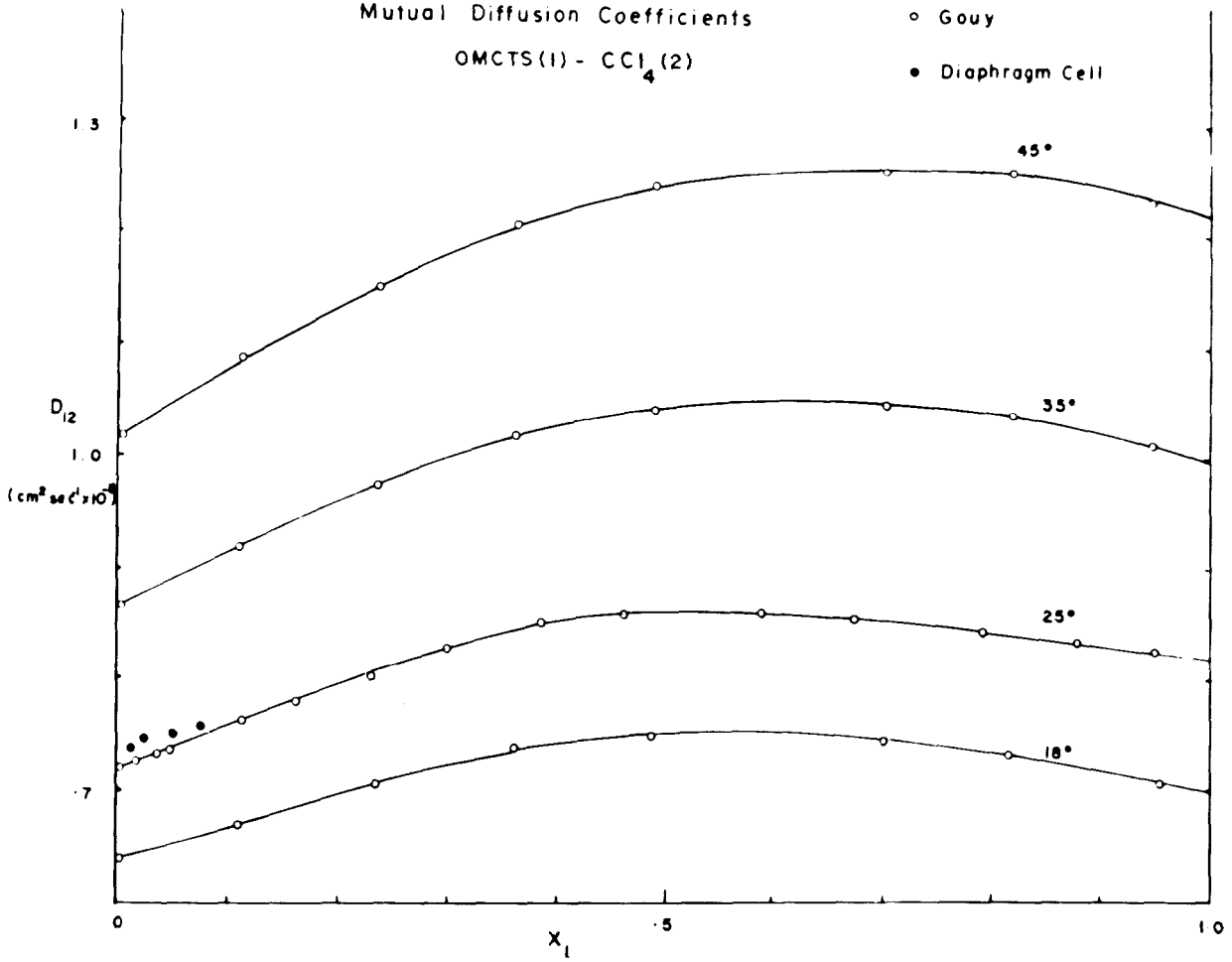


Fig. 3.5.2

Mutual Diffusion Coefficients  
OMCTS(1) -  $\text{CCl}_4$ (2)

○ Gouy  
● Diaphragm Cell



### 3.6 ACTIVITY COEFFICIENTS

The constants used in calculating activity coefficients of the volatile species are given in Tables 3.6.1 and 3.6.2. Virial coefficients for benzene were taken from Spurling's thesis<sup>98</sup>. For carbon tetrachloride the recorded virial coefficients were mutually inconsistent,<sup>99,100,101,102,103</sup> the errors in measurements being attributed to its reaction with mercury. The virial coefficients used were calculated from the equation given by Francis and McGlashan:

$$B = 575 - 2.0 \times 10^8/T^2 \quad \dots (3.6.1)$$

The noted inaccuracies in the virial coefficients limit the accuracy of the activity coefficients derived from the experimental measurements.

Experimental results are given in Appendix I. Values of  $\ln f_2$  were calculated along the lines previously suggested. In the final calculation, allowance was made for the activity of OMCTS and imperfections in the vapour phase. Activity coefficients, tabulated as  $\ln f_2$ , are listed in Tables 3.6.3 and 3.6.4.

Errors in experimental variables give rise to errors in the activity coefficients calculated from equation (2.7.1).

Errors will be considered as follows:

(1) Term(1) of equation (2.7.1)

The limitations of cathetometry were estimated at  $\pm 0.01$  mm.Hg while errors arising from temperature differences of  $0.002^\circ\text{C}$  between

successive measurements gave rise to a variable error in the pressure, having a maximum of  $\pm 0.04$  mm Hg at high temperatures and pressures. Weighings accurate to  $\pm 0.1$  mg introduced a variable error in the total concentration (vapour plus liquid) ranging from 0.03% to 0.003%. A further error occurs when calculating the mass in the vapour phase because of uncertainties in the volume occupied by the vapour phase and uncertainties in the virial coefficient. For the carbon tetrachloride-OMCTS mixtures this latter error would probably be more significant because of the greater uncertainties in the virial coefficient.

(2) Term (2) of equation (2.7.1)

The only significant errors in this term arise from uncertainties in the virial coefficients.

The overall accuracy in  $\ln f_2$  varied from approximately 0.00008 at 60°C and low OMCTS concentrations to 0.003 at 25°C and high concentrations of OMCTS.

By combining the equation suggested by Scott for the excess free energy<sup>104</sup>,

$$G^E = \frac{x_1 x_2}{1 - k(1 - 2x_1)} \sum_{n=0}^n A_n (1 - 2x_1)^n \quad \dots \quad (3.6.3)$$

where  $k$  is a skewing factor, and

$$\ln f_2 = \left( G^E - x_1 \frac{\partial G^E}{\partial x_1} \right) / RT \quad \dots \quad (3.6.4)$$

a series equation was obtained for  $\ln f_2$  which takes the form

$$\ln f_2 = \sum_{n=0}^{\infty} \frac{x_1^2 (1 - 2x_1)^{n-1}}{[1 - k(1 - 2x_1)]^2} \{A'_n [2n + 1 - 2x_1(1+n) - k(2n - 1 - 2x_1(3n - 1) + 4nx_1^2)]\}$$

... (3.6.5)

A computer programme was used to fit the activity coefficients to equation (3.6.5) - see Appendix III. Coefficients  $A'_1, A'_2, A'_3, \dots$  and the skewing factor,  $k$ , were determined after introducing a weighting function proportional to  $x_2$  as the accuracy in the activity coefficients were considered to be approximately proportional to  $x_2$ . The first three coefficients and the value of  $k$  which gave the best fit are listed in Table 3.6.5. It should be noted that for the system OMCTS - carbon tetrachloride, an error in the virial coefficient will give a constant error in the activity coefficients at any one temperature.

TABLE 3.6.1Constants for the Calculation of Activity CoefficientsOMCTS (1) - Benzene (2)

M.W. OMCTS = 296.64					
M.W. C <sub>6</sub> H <sub>6</sub> = 78.114					
Volume to reference = 118.40 ml.					
Temp (°C)	$P_1^{\circ}$	$P_2^{\circ}$	$\rho_1^{\circ}$	$\rho_2^{\circ}$	$B_{22}$
25	1.00	95.20	.9504	.8737	-1455
35	2.02	148.37	.9389	.8631	-1330
45	3.89	223.64	.9275	.8521	-1232
55	7.14	327.22	.9159	.8411	-1145
60	9.52	391.70	.9102	.8357	-1105

TABLE 3.6.2OMCTS (1)-Carbon tetrachloride(2)

M.W. OMCTS = 296.64					
M.W. CCl <sub>4</sub> = 153.839					
Volume to reference = 118.40 ml.					
Temp (°C)	$P_1^{\circ}$	$P_2^{\circ}$	$\rho_1^{\circ}$	$\rho_2^{\circ}$	$B_{22}$
25	1.00	114.23	.9504	1.5845	-1675
35	2.02	174.80	.9389	1.5650	-1531
45	3.89	259.17	.9275	1.5455	-1401
55	7.14	373.58	.9159	1.5259	-1282
60	9.52	444.21	.9102	1.5162	-1227

pressure in mm Hg, virial coeff.  $B_{22}$  in ml mole<sup>-1</sup>

Density in g/ml

TABLE 3.6.3

Activity Coefficients OMCTS (1) - C<sub>6</sub>H<sub>6</sub> (2)

Temp (°C)	x <sub>1</sub>	ln f <sub>2</sub>	Temp (°C)	x <sub>1</sub>	ln f <sub>2</sub>
25	.14420	.02432	25	.62522	.09611
35	.14450	.02242	35	.62578	.08041
45	.14495	.01911	45	.62651	.06094
55	.14541	.01655	-	-	-
60	.14576	.01539	-	-	-
25	.21140	.03995	25	.73062	.09886
35	.21183	.03401	35	.73227	.07674
45	.21235	.02972	45	.73448	.05769
55	.21319	.02571	55	.73732	.03773
60	.21365	.02364	60	.73916	.02966
25	.36362	.07159	25	.77061	.09580
35	.36517	.06194	35	.77183	.07327
45	.36739	.05353	45	.77346	.05290
55	.37019	.04358	55	.77557	.03456
60	.37149	.03999	60	.77683	.02560
25	.45132	.08320	25	.82744	.09362
35	.45276	.06927	35	.82814	.07096
45	.45450	.05796	45	.82905	.04898
55	.45714	.04678	55	.83022	.02906
60	.45859	.04145	60	.83092	.01930
25	.60166	.09461	25	.87839	.09014
35	.60347	.07811	35	.87871	.06576
45	.60590	.06044	45	.87917	.05013
55	.60915	.04526	55	.87972	.02518
60	.61094	.03836	60	.88005	.01556

TABLE 3.6.4

Activity Coefficients OMCTS (1) - CCl<sub>4</sub> (2)

Temp (°C)	x <sub>1</sub>	ln f <sub>2</sub>	Temp (°C)	x <sub>1</sub>	ln f <sub>2</sub>
25	.08603	-.00072	25	.73162	-.1170
35	.08759	-.00091	35	.73478	-.1173
45	.08949	-.00135	45	.73886	-.1206
55	.09228	-.00170	55	.74394	-.1272
60	.09404	-.00169	60	.74683	-.1309
25	.22664	-.01075	25	.79983	-.1358
35	.22930	-.01157	35	.80075	-.1373
45	.23265	-.01291	45	.80196	-.1409
55	.23735	-.01442	55	.80339	-.1437
60	.24031	-.01506	60	.80426	-.1459
25	.48426	-.05318	25	.85905	-.1509
35	.48484	-.05607	35	.85953	-.1506
45	.48559	-.05841	45	.86011	-.1539
55	.48651	-.06061	55	.86084	-.1581
60	.48707	-.06190	60	.86122	-.1606
25	.59959	-.08276	25	.38174	-.03466
35	.60283	-.08552	35	.38219	-.03544
45	.60724	-.08772	45	.38274	-.03678
55	.61272	-.09133	55	.38347	-.03851
60	.61558	-.09409	60	.38385	-.03944
25	.66796	-.09928			
35	.66906	-.10134			
45	.67052	-.10468			
55	.67242	-.10869			
60	.67359	-.11033			

Fig. 3.6.1  
 $\ln f_2$  OMCTS (1) -  $\text{CCl}_4$  (2)

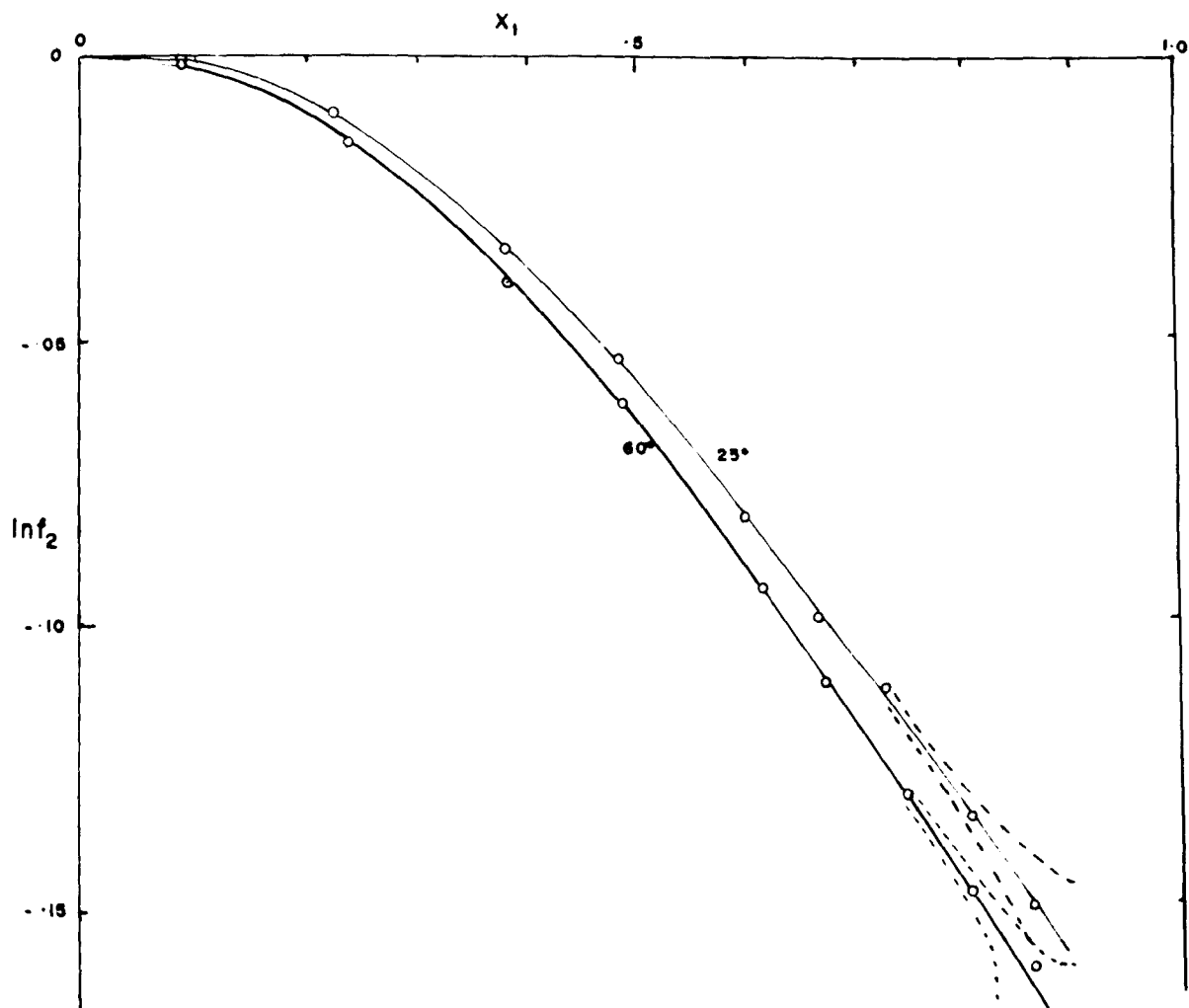


TABLE 3.6.5

Constants for Scott's Equation

Temp (°C)	<u>OMCTS - C<sub>6</sub>H<sub>6</sub></u>			k	Av. dev. in ln f <sub>2</sub>
	A' <sub>1</sub>	A' <sub>2</sub>	A' <sub>3</sub>		
25	.18714	.073859	.013782	.5	.00020
35	.14366	.082994	.001887	.5	.00054
45	.11419	.095241	.054809	.3	.00033
55	.076725	.075469	.015067	.5	.00014
60	.062057	.082133	.030608	.4	.00018
	<u>OMCTS - CCl<sub>4</sub></u>				
25	-.21517	.15493	.02273	.8	.00023
35	-.21790	.13054	.02637	.7	.00012
45	-.22130	.12947	.02694	.7	.00012
55	-.22793	.13210	.02699	.7	.00009
60	-.23177	.17895	.03528	.9	.00020